AMM Newsletter
Advanced Methods for Manufacturing

Issue 12 • September 2020

AMM Program Update

As fiscal year (FY) 2020 is ending, we reflect at the extraordinary year it was! We experienced enthusiastic recognition of the impact that advanced manufacturing can have to enable and support new reactor and component demonstrations. An AMM strategic plan was developed combining our responsibility towards AMM qualification approaches to ensure accelerated adoption and demonstration, while still ensuring long-term viability through relevant research and development of state-of-the art advanced methods of manufacturing.

Isabella van Rooyen
AMM National Technical Director

This past year, the Advanced Methods for Manufacturing (AMM) program renewed and enhanced our interaction with all our stakeholders through presentations, meetings, newsletters, and technical progress meetings. We focused efforts to reach a wider audience and stakeholder base and understand needs and gaps to improve the AMM program's strategic plan. Specifically, further collaboration with other programs will receive increased attention (as schematically shown in the figure below) and will enable the Department of Energy's Office of Nuclear Energy to be the nexus for AMM development and leadership. The stakeholder surveys response rates are currently approximately 25%, and we are aiming to increase this in FY 2021.

Mark your calendar:

- Annual AMM technical review meeting: December 2-3, 2020
- AMM qualification approaches workshop: August 2021.

For more program information, including recent publications, please visit **www.energy.gov/ne**

U.S. DEPARTMENT OF ENERGY

Cross-cutting AMM research focus areas support all major Nuclear programs across DOE, DoD, NASA, and Industry Stakeholders

NE – 5 & Other DOE NE Programs — Existing Fleet; Advanced Reactors, SMRs, & ARPs; Nuclear Battery & Micro Reactors

NNSA & NASA — Space Reactors

DoD Programs — Defense

Factory and Field Fabrication Techniques · Modular Manufacturing · Advances in Manufacturing Processes · Advances in Concrete · New Adv. Man. Tech. for Qualification and Certification to Accelerate Licensing · Advanced Integrated Fuel System Concepts

---

Congratulations to the three FY 2020 CINR awarded AMM projects:

1. HIP Cladding and Joining to Manufacture Large Dissimilar Metal Structures for Modular and GEN IV Reactors

   Principle Investigator (PI): Xiaoyuan Lou, Auburn University

   Collaborators: EPRI, Synertech P/M Inc., University of Wisconsin Madison, GE Research, GE Hitachi Nuclear Energy, Westinghouse

   Approach:
   - Integrated modeling and experimental approach
   - Economic process (decreased process steps and material costs, decrease development time)
   - Integrated near net shape HIP process: (1) thin to thick sections, (2) dissimilar materials.

2. Fiber Sensor Fused Additive Manufacturing for Smart Component Fabrication for Nuclear Energy

   PI: Kevin P. Chen, University of Pittsburgh

   Collaborators: Oak Ridge National Lab, Westinghouse Electric Company, Corning Incorporated

   Approach:
   - Embedding fiber optic sensor in laser AM-processed metals for smart component manufacturing for nuclear power systems
   - High spatial resolution measurements of T, strain, vibration, and pressures in radiation environments.

3. Diffuse field ultrasonics for in situ material property monitoring during additive manufacturing using the SMART Platform

   PI: Prof. Christopher M. Kube-The Pennsylvania State University

   Collaborators: University of North Texas; Penn State Applied Research Laboratory; State Applied Research Laboratory; Mellon University; Westinghouse Electric Company

   Approach:
   - Develop, test, and provide the essential in-situ sensing technology to achieve the outcomes of (1) rapid part quality assessment and (2) microstructural characterization during the build
   - Develop SMART (Sensing Microstructure using Acoustics in Real-Time) AM build platform
   - Correct the build process to avoid damage.

AMM funded project resulted in ASME Code case submission

D. Gandy, S. Tate, M. Albert, C. Armstrong, W. Cleary, DRAFT Code Case for 316L Stainless Steel Manufactured via Laser Powder Bed Fusion Additive Manufacturing, Submitted to ASME Boiler Pressure Vessel Code—Section III MF&E, August 19, 2020.

AMM-INDUSTRY PROJECTS
SMR Vessel Manufacture/Fabrication/Demonstration Project

David Gandy
Electric Power
Research Institute

Marc Albert
Electric Power
Research Institute

Will Kyffin
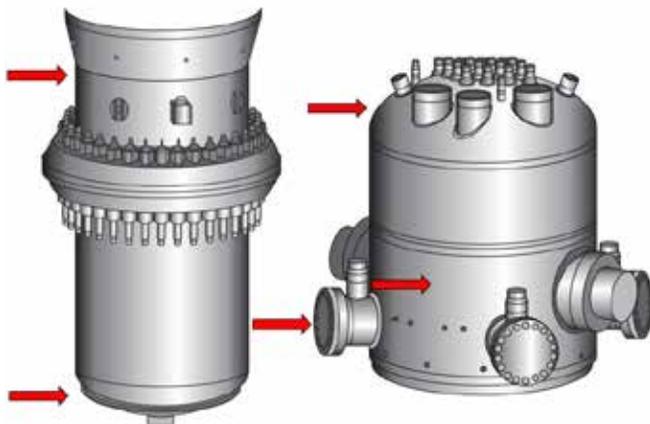Nuclear Advanced
Manufacturing
Centre

Matt Cusworth
Nuclear Advanced
Manufacturing
Centre

Keith Bridger
Bridger Welding
Engineering

Under the United States (U.S.) Department of Energy Project DE-NE0008629, the Electric Power Research Institute (EPRI), Nuclear Advanced Manufacturing Research Centre (Nuclear-AMRC), together with engineering support from NuScale Power and Synertech PM Inc., have embarked on a project to develop and produce major component assemblies of a small modular reactor (SMR) vessel at 2/3-scale using novel manufacturing technologies. The research involves the manufacture of upper and lower assemblies of the NuScale Power reactor vessel (Figure 1) using both conventional forging and powder metallurgy hot-isostatic pressing (PM-HIP) technologies, together with electron beam welding to join the component assemblies [1-4].

Figure 1. Upper and lower assemblies of the NuScale Power reactor are being assembled at 2/3-scale under this program. The arrows show components that are being produced via PM-HIP. (Photograph courtesy of NuScale Power).

The industrial team members seek to demonstrate that critical sections of an SMR reactor pressure vessel (RPV) can be manufactured and fabricated in less than 12 months and at a cost savings of more than 40% compared to today's technologies. The project aims to demonstrate and test the impact that multiple advanced manufacturing technologies can have on future production of SMRs and explore the relevance of the technologies to the production of Advanced Light Water Reactor (ALWRs), SMRs, ARs, ultra-supercritical fossil, and supercritical CO_2 plants. The project, if successful, may accelerate deployment of SMRs in both the U.S. and ultimately throughout the world.

In a previous AMM Newsletter (Issue 10) (1), early results of component manufacturing and overall tasks were described. Task 1 of the project is focused on manufacture and fabrication of the lower assembly (Figure 1, left-hand side of photograph) of the NuScale reactor at 2/3-scale (2–5). The lower assembly consists of a lower RPV head, a lower RPV flange shell, upper and lower flanges, and an upper transition shell. Each of these components will be produced and assembled by Q1-2021.

Current Status

• Produced four 2/3-scale, 1/2 diameter lower reactor heads (~70 in. (1780 mm) in diameter) via PM-HIP. (Figure 2)

• Completed machining and EB welding of a one-half diameter RPV head shell weld. (Figures 3 and 4). Note that the head was produced in two sections and welded together since a sufficiently large HIP vessel is not available to produce the entire head as one solid monolithic structure.

Continued from previous page

Figure 2. Machining of two halves of the lower head in preparation for EB welding at the Nuclear-AMRC.

- Completed a 2/3-scale diameter (~70 inches) RPV shell-to-flange mockup of a full-diameter girth weld in 47 minutes.

- Worked with major powder manufacturers to assess compositional controls to produce enhanced toughness properties consistent with forged materials.

- Manufactured four major forgings, including an upper and lower RPV flange, the lower RPV shell, and the pressurizer shell.

- Produced four RPV transition shell section (1/5th diameter) using PM-HIP. Two additional HIP capsules have been fabricated and will be filled and HIP'ed by the end of 2020.

In the next few weeks, the investigators plan to complete machining and joining of two additional lower reactor head sections via electron beam welding and complete machining and heat treatment of the upper and lower flanges and lower RPV shell. The lower flange will then be welded to the lower RPV shell and the assembly will be welded to the lower reactor head. Additionally, five sections of the upper RPV transition shell will be joined with vertical welds and then welded to the upper RPV flange in early 2021. This will complete the lower assembly (Figure 1).

Impact, Value, and Implications

If successful, the impact of the current SMR manufacturing/fabrication project will be dramatic in terms of cost reduction, quality, and schedule. The following are a few of the projected outcomes from the project:

- Demonstrate an advanced welding technology, EBW for fabrication of reactor components, which is expected to reduce welding time by 90% over conventional welding processes and methods.

- Demonstrate PM-HIP methods to manufacture difficult-to-produce sections of the SMR (upper and lower reactor heads, plenum, access covers, etc.) in as little as a few months each.

- Possibly eliminate in-service inspection requirements for no fewer than seven (out of nine) full-diameter circumferential welds using the EBW process and solution annealing.

- Develop/demonstrate diode laser cladding (DLC) technologies that can apply thin (~1 mm) layers of cladding using robotics. The overall volume of material required for cladding will be reduced by 75% resulting in a substantial cost savings across the entire vessel inner and outer clad surfaces.

Figure 3. Removal of the lower reactor head from the Nuclear-AMRC's EB welding chamber.

Continued from previous page

Figure 4. A completed EB weld joining two halves of the lower reactor vessel head. Note that the head is upside down and final machining has yet to be completed.

Acknowledgements

References

1. D. Gandy, et al., "SMR Reactor Vessel Manufacture/Fabrication/Demonstration Project," AMM Newsletter, Issue 10, October 2019, pp. 8–10.

2. D. Gandy, Factory Fabrication of SMR and AR Vessel Assemblies, GIF AMME Workshop on Advanced Manufacturing, Paris, France, February 18–19, 2020.

3. EPRI, Small Modular Reactor Vessel Manufacture and Fabrication—Phase 1 Progress, EPRI/DOE Report 3002015814, Technical Update, Electric Power Research Institute, October 2019.

4. D. Gandy, et al, "Advanced Manufacturing to Enable the Next Generation of Nuclear Plants," ANS/ICAPP 2018, Charlotte, North Carolina, April 8–11, 2018.

5. D. Gandy, et al., "Small Modular Reactor Vessel Manufacture/Fabrication Using PM-HIP and Electron Beam Welding Technologies," HIP17, 12th International Conference on Hot Isostatic Pressing, Sydney Australia, December 5–8, 2017.

6. EPRI, Innovative Manufacturing Process for Nuclear Power Plant Components via Powder Metallurgy, EPRI Report 3002008030, Electric Power Research Institute, September 2016.

7. D. Gandy, "PM-HIP Research for Structural and Pressure Retaining Applications within the Electric Power Industry," Third International Workshop on Structural Materials for Innovative Nuclear Systems (SMINS-3), Idaho Falls, Idaho, October 2013.
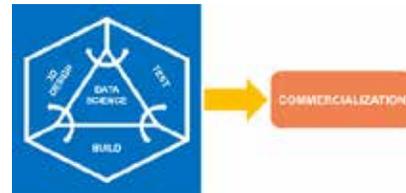
Establishment of an Integrated Advanced Manufacturing and Data Science Driven Paradigm for Advanced Reactor Systems

Scott J. Shargots, BWX Technologies, Inc.

Joseph E. Ramsey and Matthew W. Preston, BWX Technologies, Inc.

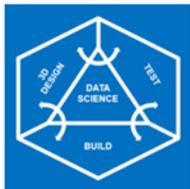**Michael Kirka, Ph.D. and Elizabeth Ellis,** Oak Ridge National Laboratory

BWX Technologies, Inc., in collaboration with ORNL, is developing the ability to implement additive manufacturing (AM) technologies, using high-temperature alloys, into the design and manufacturing of nuclear components. To accomplish this, we are establishing an integrated three-dimensional design, build, test paradigm informed by data science for advanced reactor systems. Using a combination of in-situ process monitoring technologies, modeling, and data analytics, the project aims to (1) rapidly develop the AM processing parameters for Hastelloy® X and molybdenum-based alloys for use in nuclear components and (2) demonstrate component-level qualification, leading to the certification of nuclear materials configured in complex geometries. The project scope consists of (1) conceptual design and analysis of complex nuclear component geometries; (2) AM of said complex geometries using Arcam Electron Beam Melting EBM®

Figure 1. Integrated 3D design, build, test paradigm informed by data science.

technology; (3) through in-situ monitoring, develop and refine a data science framework to create digital representations of each build; (4) use destructive and non-destructive examination and other mechanical testing to benchmark the data science framework and to demonstrate the mechanical strength of AM high temperature alloys; and (5) develop a commercialization plan for future nuclear design and manufacturing.

ID4BT
➤ Rapid Development Paradigm
➤ Technology Driven
➤ Enabling the Commercialization of High Power Dense Nuclear Designs

Reactor Design
➤ GEN IV
➤ Compact
➤ Cost Effective
➤ Inherently Safe

Advanced Materials
➤ Technology Leap
➤ Not AM Today
➤ Increased Safety Margins

Additive Manufacturing
➤ Unique Geometries
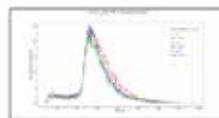➤ Improved Thermal Energy Management
➤ Customized Design
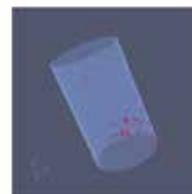
Figure 2. Description of project objectives.

Integrated Design
➤ Mechanical Design
➤ Core Physics
➤ Thermal Analysis
➤ VHTR Concept
➤ UHTR Concept

Build
➤ AM HAST® X
➤ AM Mo Alloys

Test
➤ Chemical Analysis
➤ Mechanical Tests
➤ Powder Characterization

Data Science
➤ In-situ monitoring
➤ 3D part reconstruction

Figure 3. Integrated 3D design, build, test, and data science activity descriptions.
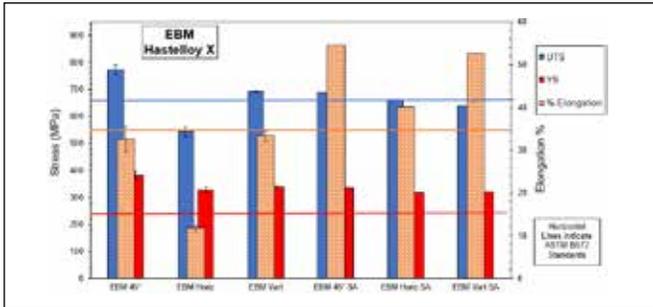
Impact and Value to Nuclear Applications

AM technologies can be transformational for the nuclear industry because they are capable of geometries not possible with conventional manufacturing techniques. Additionally, proving the ability to AM high-temperature alloys enables designs that possess improved thermal energy management, increased safety margins, and accident-tolerant characteristics. The choice of Hastelloy® X and molybdenum-based alloys bounds GEN-IV reactor technologies both in operating temperature and coolant type, which allows the results of this project to benefit a wide spectrum of GEN IV reactor designs. Additionally, a breakthrough in the proposed AM development and the integrated 3D design, build, test paradigm, with regard to molybdenum, could have an immediate impact on the current commercial reactor fleet and their endeavor for an accident-tolerant fuel design.

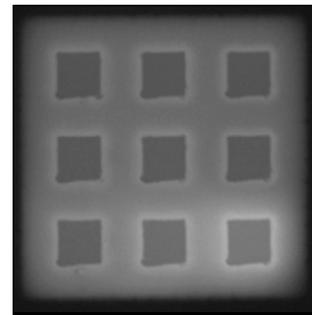**Figure 4. Arcam Spectra H installed at ORNL-MDF.**

Figure 5. 3D digital twin (red dots indicate pore detection).

Figure 6. Hastelloy® X tensile test results compared to wrought standards (each set of bars indicates build orientation).
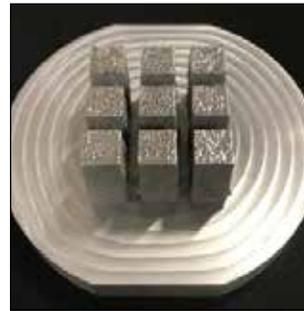

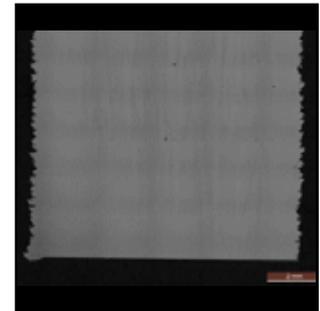
Figure 7. Hastelloy® X thin wall test builds.

Figure 8. Near-infrared image of bulk build using in-situ monitoring process.
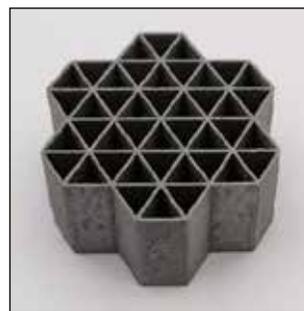
Recent Results and Highlights

As we work to close out the project, we have met all planned milestones and goals. The major successes of the BWXT and ORNL team include (1) installing the Arcam EBM® Spectra H machine (the first to be deployed in the United States); (2) successfully demonstrating the integrated 3D design, build, test paradigm; (3) successfully printing defect free Hastelloy X core components with excellent mechanical properties, excellent microstructure, and acceptable as-built surface finish and GD&T; (4) successfully printing defect-free molybdenum-based alloys with acceptable microstructure, as-built surface finish, and GD&T; (5) developing an innovative in-situ monitoring process to track build progress and inform our innovative data science platform; (6) accurately developing 3D digital twins of as-built parts; (7) developing a data science platform capable of detecting pores of 100 um or larger at 99.99% accuracy that is capable of crack detection and capable of part GD&T of +/- 90 um; and (8) developing the ability to mesh the 3D digital twin (developed by the data science platform) such that the as-built components can be analyzed to determine acceptance or rejection of defects and geometric non-conformances within the part.
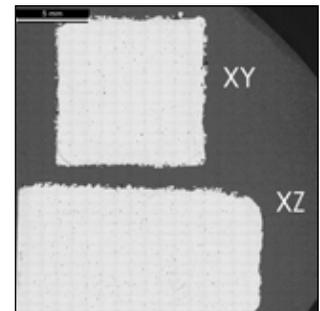

Figure 9. Molybdenum bulk test build.

Figure 10. Optical image showing no cracks or pores on molybdenum bulk builds.

Figure 11. Crack Free and pore free moly alloy unique geometry build.

Figure 12. Optical image showing no cracks or pores in moly alloy unique geometry build (← Build direction for XZ).

AMM-NEET PROJECTS
Development of Innovative Manufacturing Approach for Oxide–Dispersion Strengthened (ODS) Steel Cladding Tubes using a Low Temperature Spray Process

Kumar Sridharan
University of Wisconsin-Madison

Peter Hosemann
University of California-Berkeley

David Hoelzer
Oak Ridge National Laboratory

Stuart Maloy
Los Alamos National Laboratory

Hwasung Yeom
University of Wisconsin-Madison

State-of-the-art manufacturing routes for structural materials for advanced reactor concepts are being extensively investigated to achieve superior structural properties and improved economics. An example is the manufacture of oxide-dispersion strengthened (ODS) steels, where uniform dispersion of nanometer size-scale oxide clusters in a fine-grained ferritic steel matrix provides superior high-temperature creep strength and irradiation resistance. ODS steels can be applied to components in a variety of Generation IV reactor concepts where materials will experience higher temperatures and radiation damage levels than light water reactors. Conventional methods for manufacturing ODS steels are cost-prohibitive and involve multiple steps, including powder consolidation, and multiple hot/warm extrusion and annealing steps. Processes involving melting are not suitable for ODS steels because they can lead to upward stratification of the oxide nanoparticles.
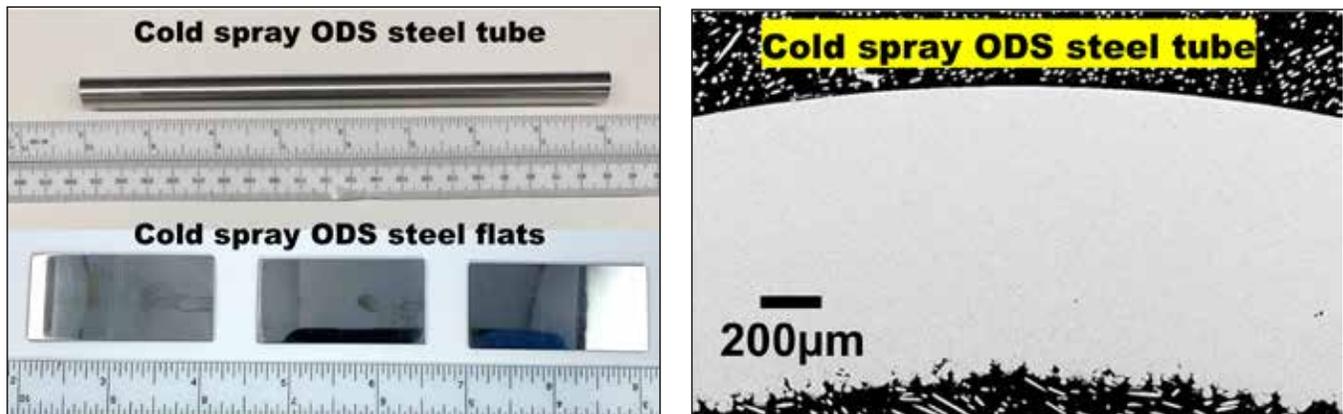
This project investigates a simpler and rapid approach of utilizing the cold spray powder spray technology for the manufacturing ODS fuel cladding tubes as an alternative to the conventional method. The process is conducive to rapid factory manufacturing and has potential to overcome the limitations of current methods in a cost-effective manner. Another phase of this project involves investigating radiation response of the cold spray manufactured ODS steel cladding tubes. Additionally, development of a cold spray process for the deposition of FeCrAl and Cr coatings on ODS steel cladding tubes manufactured by this novel method is underway to mitigate corrosion and wear in nuclear reactor materials and components.

Current Status

The feasibility of manufacturing ODS steel tubes and flats via the novel cold spray route has been demonstrated through the ongoing Department of Energy Nuclear Energy Enabling Technologies (NEET) project. The research has investigated both 14-YWT steel gas atomized powder provided by the collaborator, Oak Ridge National Laboratory. The research has involved parametric investigations of the cold spray process, including the type of propellent gas, gas pre-heat temperature, powder size distribution, and composition, as well as post-deposition thermal treatments to achieve high-quality ODS steel material with flat and cladding tube geometries, as shown in Figure 1. As also shown in this figure, the ODS tube wall thickness was about 1.2 mm, which was achieved in a single-pass deposition process. Image analysis revealed a porosity level of 0.03%. Additionally, the ferritic steel phase in the feedstock powder was preserved in the as-manufactured ODS steel material without formation of additional oxide phases. We are presently investigating cold spray deposition with ball-milled powders provided by the collaborator, Los Alamos National Laboratory. These powders have a superior microstructure, but they are also larger in size and are in a work-hardened state. To overcome this challenge, we are investigating cryomilling to reduce particle size followed by annealing to reduce powder particle hardness.
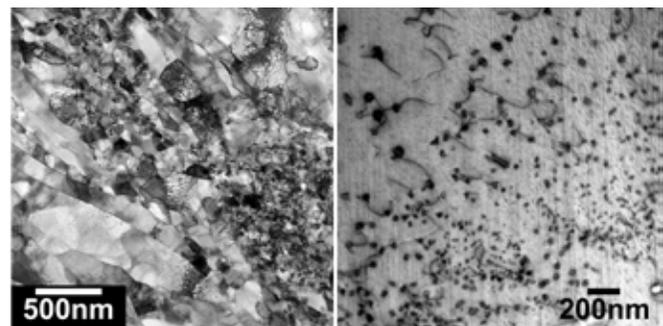
Figure 1. (left) Photographs of an ODS steel tube and ODS steel flats manufactured by cold spray process and (right) SEM cross-sectional image of the ODS steel tube manufactured by this process.

In-depth microstructural characterization of the ODS cladding was performed using both scanning electron microscopy (SEM) and scanning/transmission electron microscopy (S/TEM). STEM examination of the as-deposited ODS steel material showed a typical severe plastic deformation microstructure. As shown in Figure 2, the microstructure exhibited inhomogeneous grain size distribution with a size range of tens of nanometers to hundreds of nanometers, resulting from grain refinement during dynamic recrystallization in the cold spray process. In addition, some fine grains showed a high density of dislocation structure. Fe-Y intermetallic nanoparticles that were observed in the feedstock powder particles by high-resolution imaging were not observed in the cold spray tubes, likely due to their dissolution into matrix during the high-velocity impact and deformation of the particles on the substrate surface. Post-deposition heat treatment in partial vacuum of the as-deposited materials was conducted in the temperature range of 800°C to 1100°C to achieve further densification of the as-fabricated ODS steel material and precipitation of oxide nanoparticles. The heat treatment resulted in decrease of porosity level and precipitation of high number density oxide nanoparticles in grains and grain boundaries, as shown in Figure 2. TEM-EDS elemental analysis confirmed these nanoparticles to be TiO_2 (50 nm to 150 nm size) and Ti-Y-O particles (20 nm to 80 nm size). The grain size ranged from 4 µm to 8 µm, which is higher than conventionally processed ODS steel. Arrangements are being made for tensile testing of these samples using miniature test specimens to bench-mark the cold spray manufactured ODS steel cladding tubes to the ODS steel cladding tubes manufactured by the conventional route.
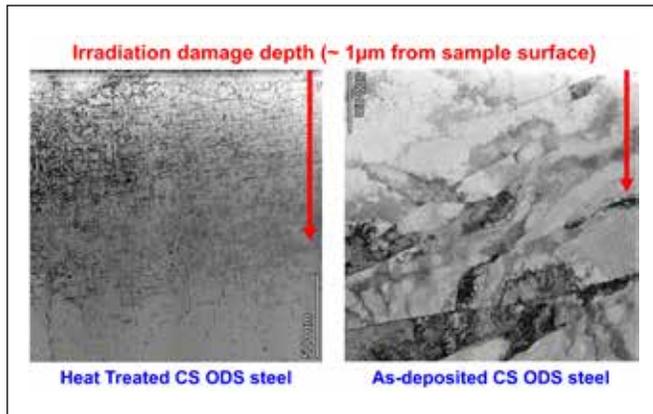
Heavy ion irradiations and post-irradiation characterization for two distinctly different manufacturing routes (cold spray process and conventional mechanical alloying and multiple extrusion) have been performed at University of Wisconsin-Madison and Idaho National Laboratory. This specific study was supported by Rapid Turnaround Experiment in the Nuclear Science User Facilities program. ODS steel samples with three conditions (as-fabricated cold spray ODS steel, heat-treated cold spray ODS steel, and conventionally manufactured ODS steel) were irradiated at the University of Wisconsin's Ion Beam Laboratory using a 3.7-MeV rastered heavy ion beam (Fe^{+2} ion) to induce a peak damage level of up to 110 dpa. The flux and dpa rate during irradiation were 4.2×10^{12} ion/cm²s and 4.7×10^{-3} dpa/s. The irradiation damage profile was simulated using SRIM "Quick" Kinchin-Pease model, which showed the dpa peak under these irradiation conditions to be about 1 µm below the surface. The sample temperature was 500°C and closely monitored using thermocouples welded on sample stage. TEM lamella fabrication and STEM characterization

Figure 2. TEM images of (left) as-deposited ODS steel tube and (right) ODS steel tube after heat treatment at 1100°C for 1 hour in partial vacuum.

Figure 3. BF TEM image of (left) heat-treated cold spray ODS steel and (right) as-deposited cold spray ODS steel after the ion-irradiation experiment.

were performed at the University of Wisconsin, Madison's Nanoscale Imaging and Analysis Center (UW-NIAC) and the Irradiated Material Characterization Laboratory at Idaho National Laboratory. These studies indicated that for all three samples, coarse oxide nanoparticles in size range of 10 nm to 80 nm were unstable at this high irradiation damage level and dissolved back into the matrix. As shown in Figure 3, the heat-treated cold spray ODS samples showed a high density of <100> type dislocation loops and line dislocation structures in the damaged region but these defects were not clearly identified in the as-fabricated cold spray samples. High sink strength of the material associated with fine grain structure and pre-existing line dislocations may have contributed to the radiation damage resistance.

Finally, a parallel effort on applying the cold spray process to manufacture functionally graded ODS steel tube for enhancing corrosion/oxidation resistance was conducted. Examples of this effort are ODS steel tube cladding tubes coated with oxidation-resistant materials FeCrAl ($Fe_{20}Cr_5Al$) and Cr, also by the cold spray process. Oxidation experiments conducted at 1000°C for the FeCrAl-coated claddings showed significantly superior oxidation resistance compared to the uncoated ODS cladding tubes. The end result is a highly oxidation-resistant ODS steel cladding tube produced in a rapid cost-effective manner entirely by the cold spray process.

Conclusions

This research program has explored a novel manufacturing approach for ODS steel fuel cladding tubes using cold spray technology as an alternative to the conventional manufacturing method, which requires mechanical alloying, multiple extrusions, and annealing steps. With considerable optimization of cold spray parameters, free-standing ODS steel cladding tubes with diameter and wall thickness prototypical to actual fuel cladding was successfully manufactured. A series of post-deposition heat treatments were investigated to precipitate the oxide nanoparticles and densify the microstructure. Heavy ion irradiation of the cold spray manufactured ODS steel and conventional ODS steel has been performed to understand the role of manufacturing process on irradiation damage. Finally, dual-material system consisting of ODS coated with FeCrAl or Cr was developed using the cold spray process for enhancing the high-temperature oxidation resistance of the ODS steel cladding tube.

Acknowledgement

References

1.   B. Maier, et al., A Novel Approach for Manufacturing Oxide Dispersion Strengthened (ODS) Steel Cladding Tubes using Cold Spray Technology, Nuclear Engineering and Technology, Vol. 51, pp. 1069–1074, 2019.

2.   M. Lenling, et al., "Manufacturing Oxide Dispersion Strengthened (ODS) Steel Fuel Cladding Tubes using the Cold Spray Process," JOM, Vol. 71, No. 8, pp. 2868–2873, 2019.

3.   H. Yeom and K. Sridharan, "Recent advances of cold spray technology in nuclear energy applications," Advanced Materials and Processes (invited), July 2020.

4.   H. Yeom and K. Sridharan, "Cold Spray Technology in Nuclear Energy Applications: A Review of Recent Advances," Annals of Nuclear Energy (accepted in press), 2020.
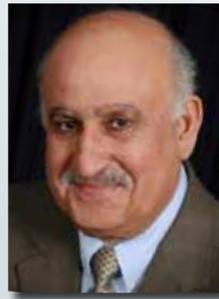
Machine Learning–based Processing of Thermal Tomography Images for Automated Quality Control of Additively Manufactured Stainless Steel and Inconel Structures

Alexander Heifetz
Argonne National Laboratory

Xin Zhang
ANL & IIT

Jafar Saniie
Illinois Institute of Technology

William Cleary
Westinghouse Electric Company

Additive manufacturing (AM) is an emerging method for cost-efficient production of low-volume custom and unique parts with minimal supply-chain dependence. In particular, AM potentially provides a cost-saving option for replacing aging nuclear reactor parts and reducing costs for new construction of advanced reactors. Metals of interest for passive structures in nuclear applications typically include high-strength corrosion-resistant stainless steel and nickel super alloys. Because of high strength, shape forming of these metals into complex geometry structures is not trivial. AM of such metals is currently based on laser powder-bed fusion (LPBF). Because of the intrinsic features of LPBF, material defects such as porosity and anisotropy can appear in the metallic structure. A pore is potentially a seed for crack formation in the structure due to thermal and mechanical stresses in nuclear reactor. Quality control (QC) in AM involves detection of material flaws in real-time during manufacturing, and non-destructive evaluation (NDE) of the structure after manufacturing. Currently, there exist limited options for nondestructive examination (NDE) of AM structures either during or post-manufacturing. Deployment of high-resolution NDE systems, such as X-ray tomography, is limited by spatial constraints of the metal 3D printer, large size and complex shapes with lack of rotational symmetry of the AM parts. Contact NDE techniques, such as ultrasound, face challenges because AM structures have rough surfaces that affects probe coupling. and the techniques require time-consuming point-by-point raster scanning of specimens.

As a solution to NDE of AM structures, we are developing pulsed thermal tomography (PTT) algorithms for 3D imaging and material flaw detection. The method is non-contact and scalable to arbitrary structure size. A schematic depiction of the PTT setup is shown in Figure 1. The method consists of illuminating material with a white light flash lamp, which rapidly deposits heat on the material surface. Heat transfer then takes place from the heated surface to the interior of the sample, resulting in a continuous decrease of the surface temperature. A megapixel fast frame infrared (IR) camera records thermograms—time-resolved images of surface temperature distribution $T(x,y,t)$. Thermal tomography obtains reconstruction of 3D spatial effusivity $e(x,y,z)$ from the data stack of thermography images.

Neural Learning-based Blind Source Separation in Thermal Images

Detection of fine features in thermal images is limited by IR camera thermal noise, non-uniform heating of the specimen, and blurring due to diffusion. The objective of this study is to investigate the application of unsupervised machine learning (ML) for enhancement of thermal images. We have developed a Neural Learning-based Blind Source Separation (NLBSS) algorithm, which separates
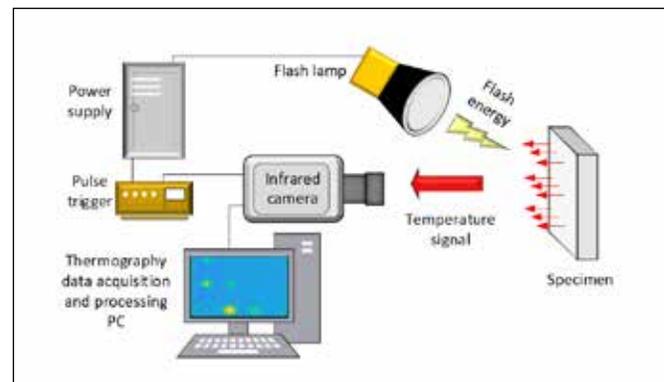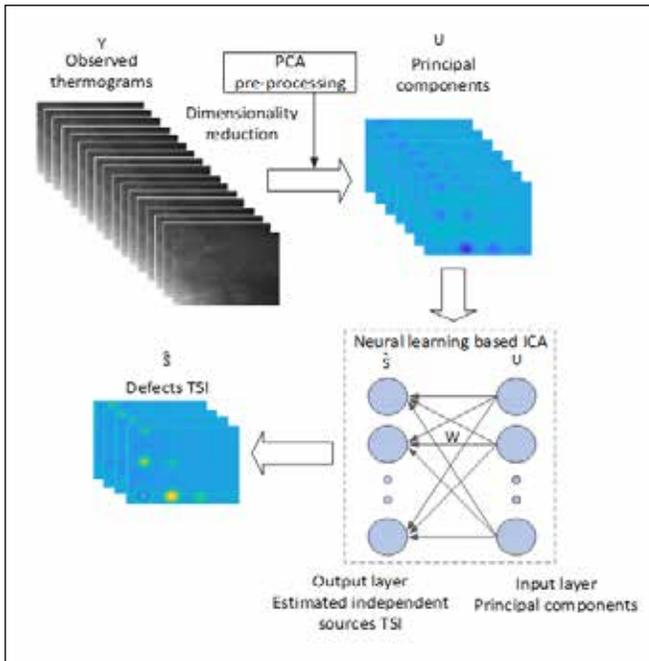

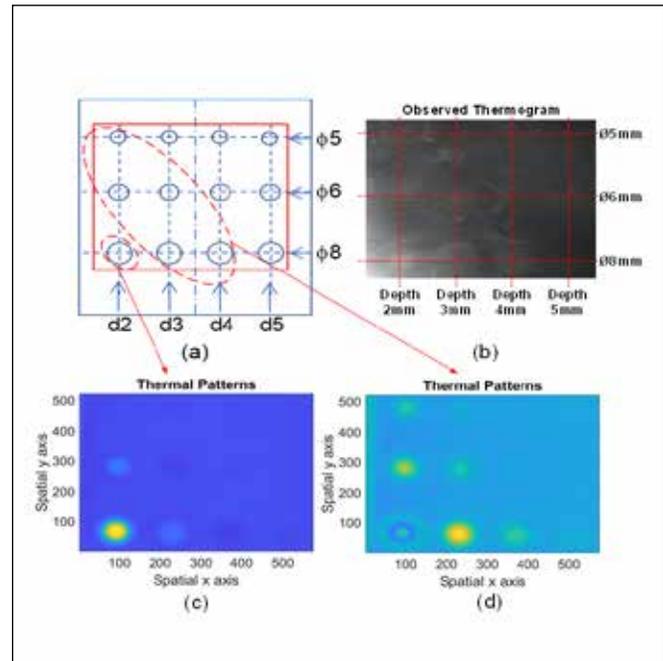**Figure 1. Schematics of pulsed thermal tomography system [1].**

Continued from previous page

Figure 2. Flowchart of Neural Learning-based Blind Source Separation algorithm [1].

Figure 4. Detection of smaller-diameter imprinted defects in SS316L plate with NLBSS [1]

defects from the background without using any a-priori information about the source of signals [1,2]. The principle of NLBSS is shown in the flowchart in Figure 2. Each segment of the thermograms recorded with PTT exhibits different temperature evolution during the transient response so that each source signal contributes to the Thermal Source Image (TSI). In NLBSS, we use Principal Component Analysis (PCA) to extract main features of thermography data, which reduces thermal imaging noises and artifacts. Next, the Independent Component Analysis (ICA), implemented in a two-layer neural network structure, is applied to automatically separate image regions containing signatures of material defects from image regions that do not contain any material flaws. The neural network structure utilizes the fast fixed-point algorithm for optimization to speed up the defect detection. This approach is computationally simple and requires little memory space.

Performance of the NLBSS algorithm was demonstrated on experimental thermography data obtained from imaging stainless steel 316L plates fabricated with the LPBF method. Defects consisting of hemispherical porosity regions containing un-sintered metallic powder were imprinted into the plates during fabrication using a sterelithography (STL) file with a drawing of the pattern of hemispherical inclusions. The design is shown in Figure 4(a) for one set of the embedded calibrated internal defects. The dimensions of the plate are Length×Width×Thickness:

152 mm×76 mm×10 mm. The defects have diameters of 5 mm, 6 mm, 8 mm, and located at depths of 2 mm, 3 mm, 4 mm, and 5 mm. For example, the labelling scheme in Figure 4(a) is such that the defect with diameter of 8 mm, located at depth of 5 mm, is represented as defect ($\varnothing$8,d5). An example of a recorded raw image is shown in Figure 4(b). Results of image processing and defect detection using NLBSS algorithm are shown in Figures 4(c) and 4(d). The defects detected in this experiment are indicated with dashed line ovals in Figure 4(a). In particular, Figure 4(c) clearly shows the defect ($\varnothing$8,d2), and Figure 4(d) shows the defects ($\varnothing$8,d3), ($\varnothing$8,d4), ($\varnothing$6,d2), ($\varnothing$6,d3), and ($\varnothing$5,d2). The defects ($\varnothing$5,d3), ($\varnothing$6,d4), and ($\varnothing$8,d5) are detected with relatively lower confidence.

The experiment was repeated to detect smaller defects in the AM plate. The imaged area of the plate is indicated with a red box in Figure 6(a). Figure 6(a) shows smaller defects with diameters of 4 mm, 3 mm, 2 mm, and 1 mm, and located at depth of 1 mm, 2 mm, 3 mm, 4 mm, and 5 mm. Figure 6(b) shows the raw thermogram image recorded with IR camera. After processing the thermograms with the NLBSS algorithm, Figures 6(c) shows enhanced contrast of defects ($\varnothing$4,d1), ($\varnothing$3,d1), ($\varnothing$2,d1), and weak ($\varnothing$1,d1). Figure 6(d) shows defects ($\varnothing$4,d2), ($\varnothing$3,d2), and ($\varnothing$2,d2). Detected defects are indicated in Figure 6(a) with dashed line ovals.
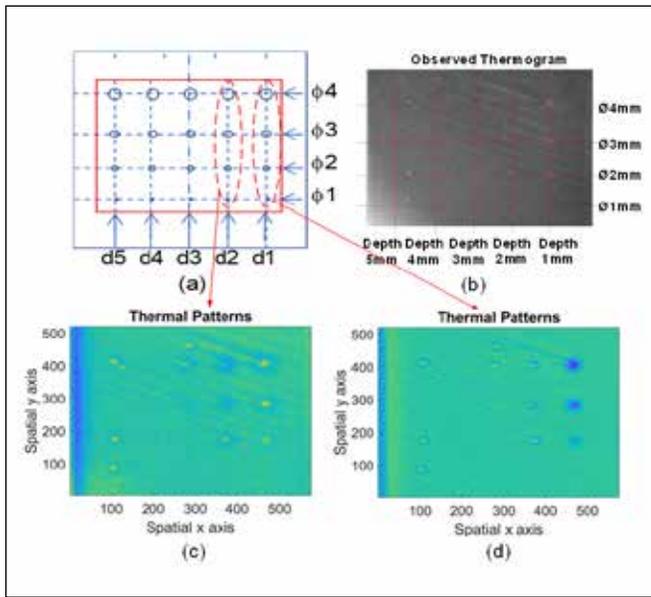
Continued from previous page

Figure 4. Detection of smaller-diameter imprinted defects in SS316L plate with NLBSS [1]

Sparse Coding with Discrete Cosine Transform Removal of Additive White Gaussian Noise from Thermal Images

While high-resolution thermal images can be obtained from cooled semiconductor detector IR cameras, there exist less-expensive and smaller form factor microbolometer detector IR cameras. Thermal images obtained with a compact IR camera have lower quality, as compared to those obtained with a high-end cooled semiconductor IR camera, because of lower sensitivity, lower sampling rate, and strong noises of small IR camera. Reduction in image quality can be partially compensated with machine-learning-based image de-noising algorithms [3]. We model IR camera noises using the Additive white Gaussian noise (AWGN) model. In principle, AWGN can be removed from images with a Gaussian filter, but this leads to image blurring. We show that the quality of images is enhanced using unsupervised machine learning (ML) Sparse Coding (SC) and Discrete Cosine Transform (DCT) ML algorithms, which remove AWGN without blurring the images.
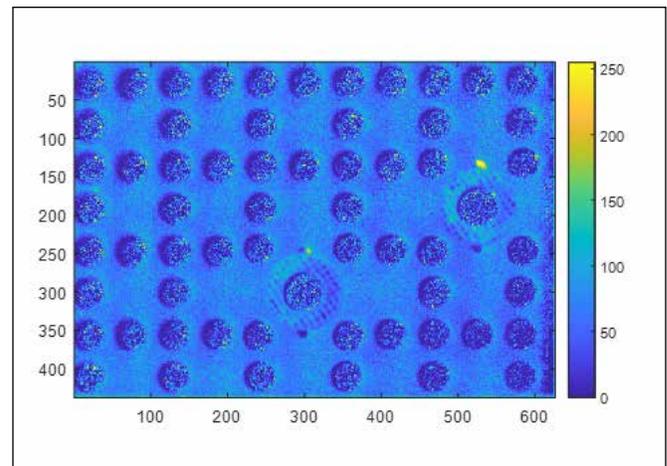

Figure 5. (Left) Laboratory PTT system using high-end IR camera. (Right) Reconstructed parallel plane slice at 1-mm deep.
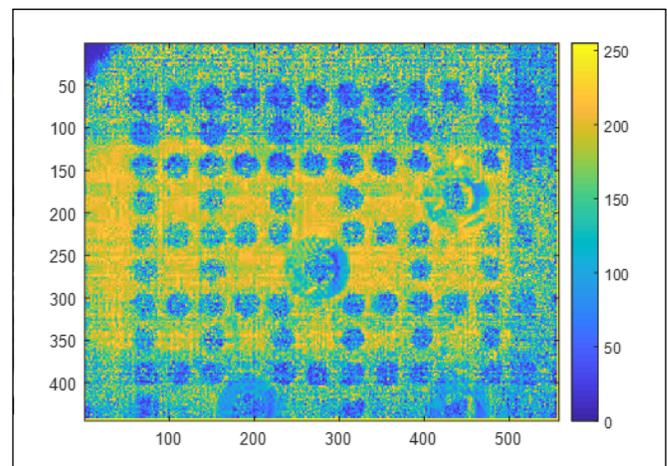

Figure 5. (Left) Laboratory PTT system using high-end IR camera. (Right) Reconstructed parallel plane slice at 1-mm deep.

Continued from previous page

This approach is demonstrated through imaging of an Inconel 718 nozzle plate fabricated with LPBF method. The plate is 17 mm thick, and the imaged area is approximately 90 mm × 60 mm. Figure 5 shows a photograph of a laboratory thermal tomography system using high-end FLIR x8501sc camera, and the image of reconstructed effusivity in the horizontal plane at 1 mm deep. Figure 6 shows a photogram of a laboratory thermal tomography system using compact lower-cost FLIR A65 camera, and corresponding image of reconstructed effusivity in the horizontal plane at 1 mm deep. Figure 6 is an image of the reconstructed effusivity processed with an SC/DCT algorithm to remove AWGN. While the imaging quality in Figure 6 is lower than that of Figure 5, essential features of the AM structure can be seen in the image in Figure 6.

Conclusion

Our results indicate that unsupervised ML-based algorithms can be used for enhancement of thermography and thermal tomography images. Experimentally detected smallest flaw size is a 1 mm-diameter hemispherical-shaped porosity region, located 1 mm below the plate surface. Future work will investigate detection of smaller-size flaws in AM structures. In addition, ML algorithms will be developed for improved compensation in noises and decreased resolution due to imaging hardware based on low-cost compact IR cameras.

References

1. X. Zhang, J. Saniie, A. Heifetz, "Neural learning based blind source separation for detection of material defects in pulsed thermography images," accepted at IEEE Conference on Electro-Information Technology, EIT 2020.

2. A. Heifetz, X. Zhang, J. Saniie, D. Shribak, T. W. Elmer, B. Saboriendo, S. Bakhtiari, W. Cleary, Imaging of Calibrated Defects in Additively Manufactured Materials, ANL-20/23, Argonne National Laboratory, 2020).

3. A. Heifetz, X. Zhang, J. Saniie, B. Khaykovich, Development of Thermal Tomography Imaging System for In-Service Nondestructive Evaluation of Additively Manufactured Components, ANL-20/46, Argonne National Laboratory, 2020.

AMM-NEET-NSUF PROJECTS
Enhancing irradiation tolerance of steels via nanostructuring by innovative manufacturing techniques

This project involves neutron irradiation and post-irradiation examination of bulk nanostructured SS304 and SS316 (austenitic), Grade 91 (ferritic/martensitic, F/M) and ferritic FeCrAl steels that are anticipated to have enhanced irradiation tolerance and are produced by two innovative, low-cost manufacturing techniques, equal-channel angular pressing (ECAP) and high-pressure torsion (HPT). The objectives of this research are to establish/enhance our fundamental understanding of irradiation effects in ultrafine-grained (UFG, 100 nm < grain diameter < 1 μm) or nanocrystalline (NC, grain diameter < 100 nm) steels produced by ECAP or HPT, and to assess the potential applications of ECAP and HPT in fabricating materials for applications in current and advanced reactors. Improving the performance of currently used austenitic, F/M, and ferritic steels through microstructural engineering via advanced manufacturing techniques provides high potential to improve radiation tolerance at relatively low cost compared to development of new alloys.

ECAP and HPT produce ultrafine or NC grain sizes in metals and alloys through application of severe plastic deformation. It is relatively simple to perform ECAP and HPT at relatively low cost. Figure 1 shows the schematics of ECAP and HPT. Alloys produced by ECAP or HPT possess

Haiming Wen
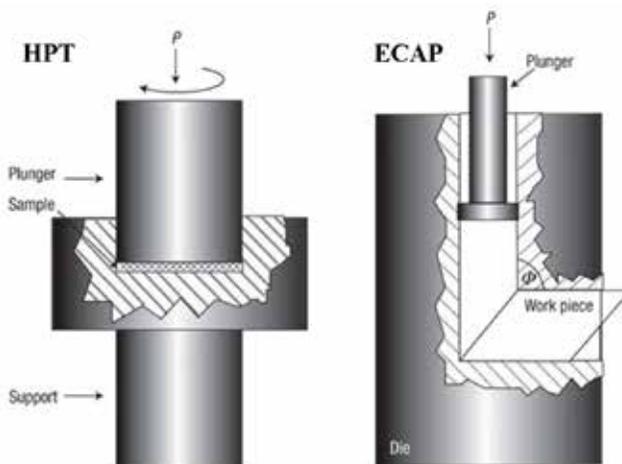Missouri University of Science and Technology

dramatically higher strength than their conventionally processed counterparts, owing to significant grain boundary (GB) strengthening, and are anticipated to have significantly enhanced irradiation tolerance due to significant volume fraction of GBs that serve as sinks or recombination centers for radiation-induced defects. Austenitic steels are very important core-internal materials for light-water reactors (LWRs), F/M steels are leading fuel cladding and structural materials for advanced fast reactors, and FeCrAl steels are candidate materials for accident-tolerant fuel cladding in LWRs. Life extension of LWRs and development of fast reactors require steels with enhanced irradiation tolerance and higher strength. UFG or NC austenitic, F/M, or ferritic steels have not been neutron irradiated, and their performance under neutron irradiation is not established. This work will establish the performance of UFG and NC variants of reactor structural and cladding steels produced by ECAP or HPT, under neutron irradiation at relevant reactor operating temperatures. Our project is focused on pre-irradiation characterization, neutron irradiation and post-irradiation examination of UFG or NC austenitic, F/M, and ferritic steels; these materials have been produced by our collaborators using ECAP or HPT.

Impact and Value to Nuclear Applications

The outcomes of this research will be a feasibility assessment of the application of two low-cost advanced manufacturing techniques (ECAP and HPT) in fabricating materials with improved performance for current and advanced reactors, with an established/enhanced understanding of the irradiation effects in UFG and NC austenitic, F/M, and ferritic steels. The application of low-cost advanced manufacturing techniques to improve the performance of currently used materials in LWRs and advanced reactors using microstructural engineering will contribute to the life extension of LWRs and expedite the development of advanced fast reactors. Hence, the research is anticipated to have significant impacts on nuclear energy research and development.

Current Status

The microstructure and mechanical properties of the bulk nanostructured steels manufactured by ECAP and HPT have been thoroughly characterized. The steels manufactured by ECAP typically have an average grain size of ~400 nm, whereas those manufactured by HPT mostly have an average gain size of ~100 nm. An example

Figure 1. Schematic of equal-channel angular pressing and high-pressure torsion.
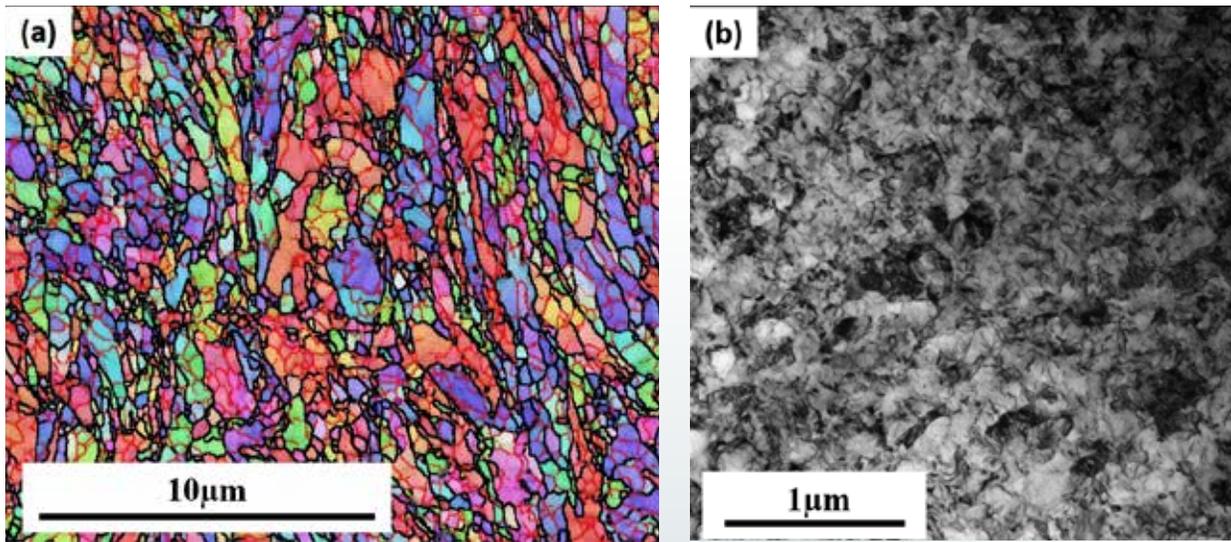
Figure 2. (a) Electron backscatter orientation map of ECAP Grade 91 steel; (b) transmission electron microscopy image of HPT Grade 91 steel.

of the microstructure is shown in Figure 2. The strength/hardness of ECAP-manufactured steels is typically ~1.5–2 times that of their conventionally manufactured coarse-grained counterparts, and the strength/hardness of HPT manufactured steels is typically ~2–3 times that of their conventionally manufactured coarse-grained (CG, grain diameter >1 μm) counterparts (see Figure 3). Any pre-existing second-phase particles/precipitates (for example, those carbides and nitrides in Grade 91 steel) have been characterized in detail using advanced microstructural characterization techniques.

A significant part of the pre-irradiation characterization also included understanding the thermal stability of the bulk nanostructured steels produced by ECAP and HPT. Metals and alloys fabricated using ECAP and HPT consist of high GB energy and strain energy, which act as driving forces for grain growth and recrystallization, respectively. It is also important to understand the thermal stability of these materials to exclude the thermal effects during elevated-temperature irradiation. UFG (produced by ECAP) and NC (produced by HPT) SS304, SS316, Grade 91 and FeCrAl (Kanthal-D) steels were
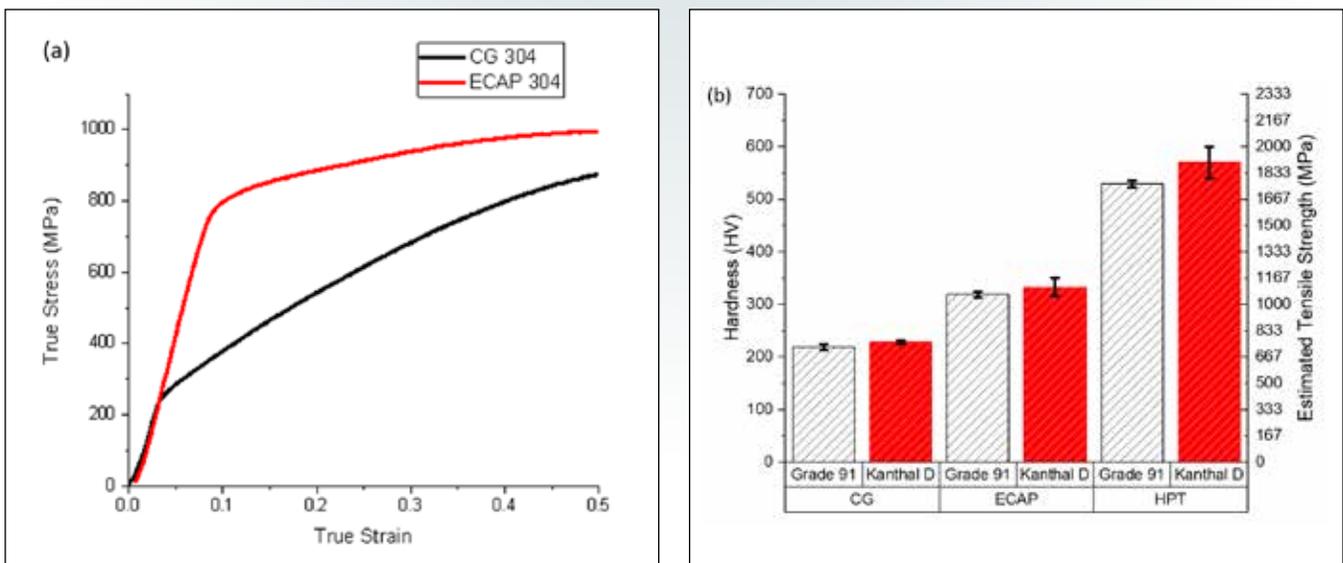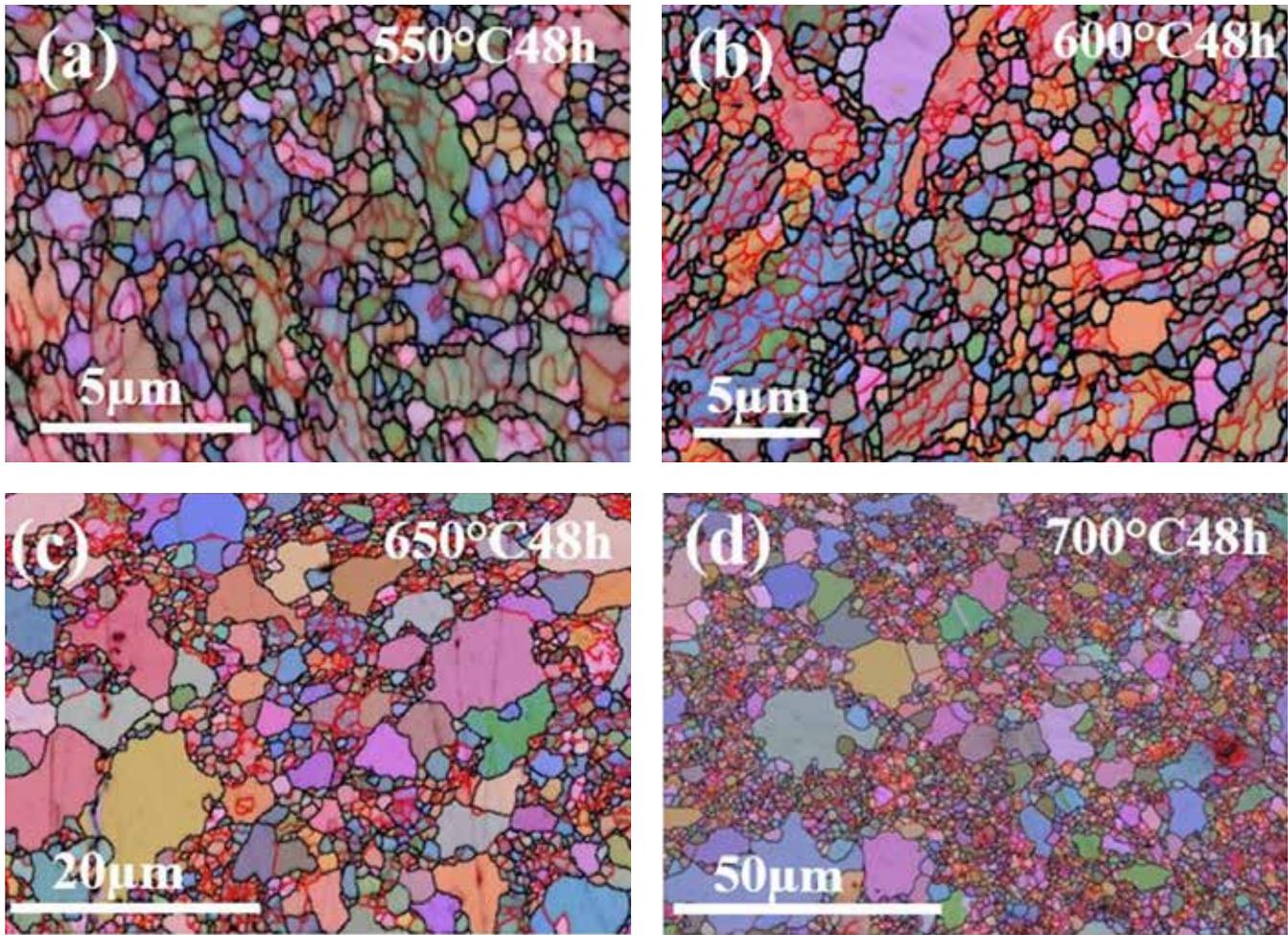

Figure 3. (a) Compressive true stress-strain curves of ECAP and coarse-grained SS304; (b) Vickers hardness of ECAP and HPT Grade 91 and Kanthal-D.
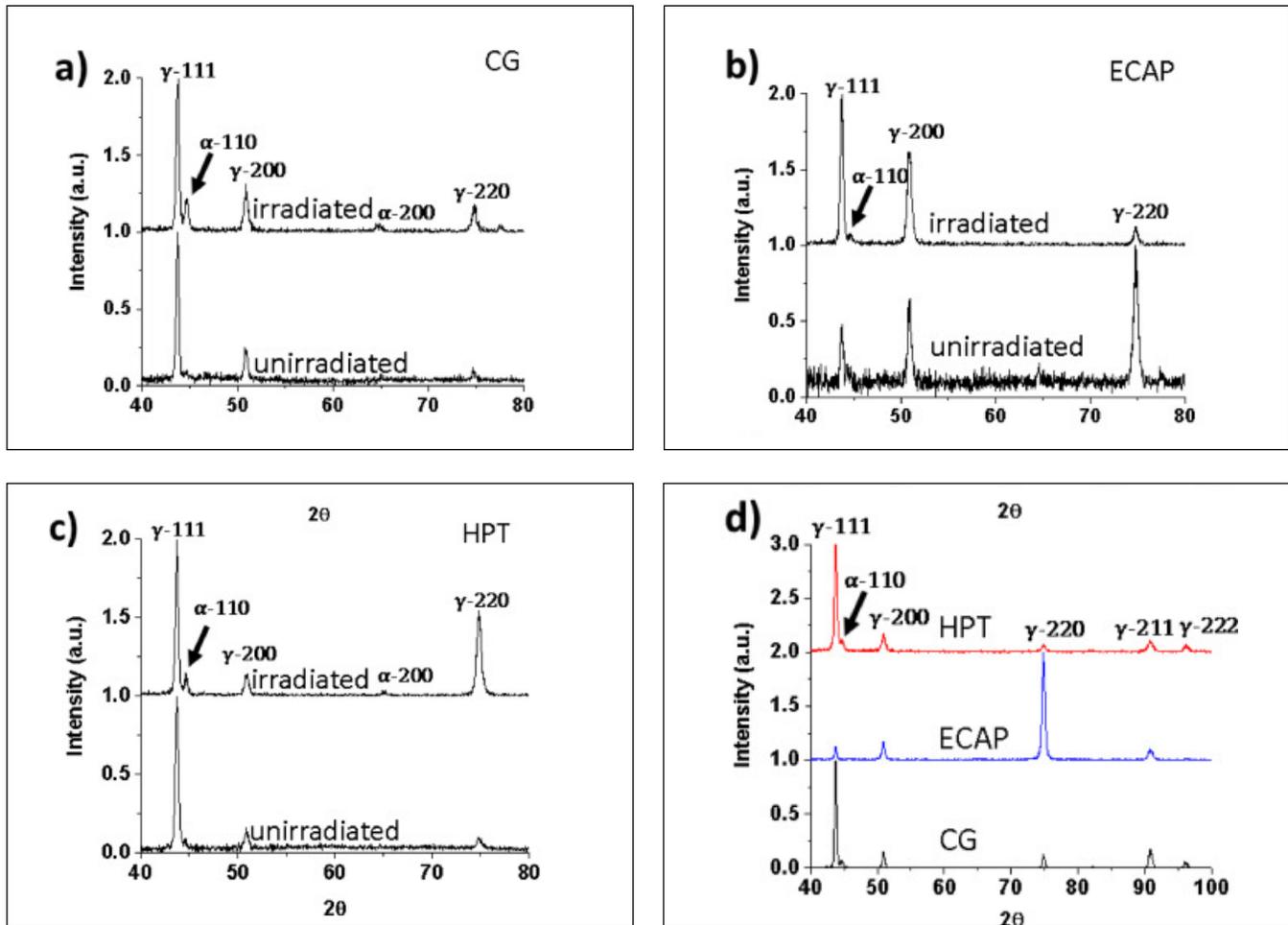
Figure 4. Electron backscatter diffraction orientation maps of the ECAP-manufactured Grade 91 after 48 h of annealing at (a) 550°C, (b) 600°C, (c) 650°C, and (d) 700°C.

annealed at different temperatures for different times, and Vickers microhardness measurements and electron backscatter diffraction maps were obtained after each of the annealing conditions. See Figure 4 for an example. It was found that ECAP processed specimens possessed a higher thermal stability than HPT specimens. This improved thermal stability in ECAP-manufactured steels is attributed to the increased volume fraction of low-angle GBs (with associated lower GB energy) stabilizing the grain structure. Low-angle GBs are a result of early stages of grain refinement. To summarize the results on thermal stability studies, both ECAP and HPT 304 samples are thermally stable up to 600°C, ECAP 316 is stable up to 600°C, HPT 316 is stable up to 500°C, ECAP Grade 91 is stable up to 550°C, HPT Grade 91 is stable up to 500°C, ECAP Kanthal-D is stable up to 550°C, and HPT Kanthal-D is unstable above 500°C.

Bulk nanostructured SS304, SS316, Grade 91 and Kanthal-D steels manufactured by ECAP and HPT, along with their conventionally manufactured CG counterparts, have been neutron irradiated in the Advanced Test Reactor (ATR) at Idaho National Laboratory. The irradiation conditions include two temperatures (300 and 500°C), and two neutron dose levels (2 and 6 displacements per atom [dpa]). The irradiation capsules with 2 dpa specimens have come out of the reactor, and they are being shipped from ATR to the Hot Fuel Examination Facility. The disassembly of the capsules and cataloging of the specimens will take place in November or December 2020. After that, the post-irradiation examination will begin, which will include mechanical testing and detailed microstructural examination.

Continued from previous page

Figure 5. (a–c) Grazing incidence XRD and gonio scans showing the ion irradiated thin film region and non-irradiated bulk of the CG, ECAP, and HPT 304L. A significant amount of α-ferrite is seen in CG and HPT 304L after irradiation as evident from the α-110 reflection. (d) XRD patterns of CG, ECAP, and HPT 304L after annealing at 500°C for 24 hrs.

During the long time for neutron irradiation, Nuclear Science User Facilities (NSUF) – Rapid Turnaround Experiments (RTE) projects have been leveraged to benefit this NEET-NSUF project. The RTE projects involved ion irradiation and post-irradiation examination of the bulk nanostructured steels. The ion irradiation results will eventually be compared against neutron irradiation results. For example, self-ion irradiation was carried out using a raster beam of 3.7 MeV Fe2+ ions on CG, ECAP, and HPT 304 up to 50 dpa. Grazing incidence X-ray diffraction (GIXRD) and gonio scan were performed to get information on the phases present in the irradiated region and the unirradiated bulk region. An α-110 peak was observed in GIXRD pattern obtained from the irradiated region in CG, ECAP, and HPT 304 as opposed to the gonio scans of the bulk sample (Figure 5). A small α-110 peak of very low intensity was observed in the gonio scans, which can be a result of the thermal effects (Figure 5d) or the contribution from the irradiated surface layer. It was clearly indicated

from the GIXRD patterns that irradiated ECAP and HPT 304 had significantly less amount of ferrite compared to irradiated CG 304. To get more accurate phase fractions, a precession electron diffraction (PED) was performed. It was determined that the phase fraction of ferrite in irradiated CG, ECAP, and HPT 304 were 33%, 6.5%, and 2%, respectively, as can be seen in Figure 6. These results clearly indicated that bulk nanostructured 304 is more resistant to irradiation-induced ferritic transformation as compared to CG 304. In addition, detailed atom probe tomography (APT) study indicated that irradiation-induced segregation (RIS) is significantly reduced in the NC grains, as compared to that in the ultrafine grains (Figure 7). Therefore, as the grain size is decreased, the irradiation resistance is enhanced. The enhanced resistance of nanostructured 304 to irradiation-induced ferritic transformation is attributed to reduced irradiation-induced strain and RIS. Ion irradiation of the other grades (Kanthal-D and G91)
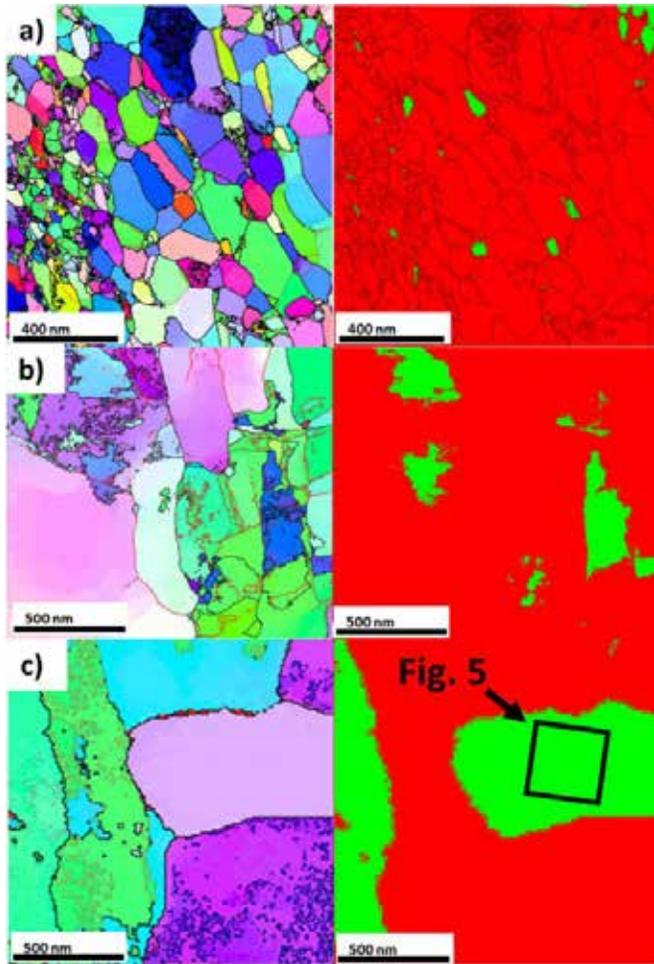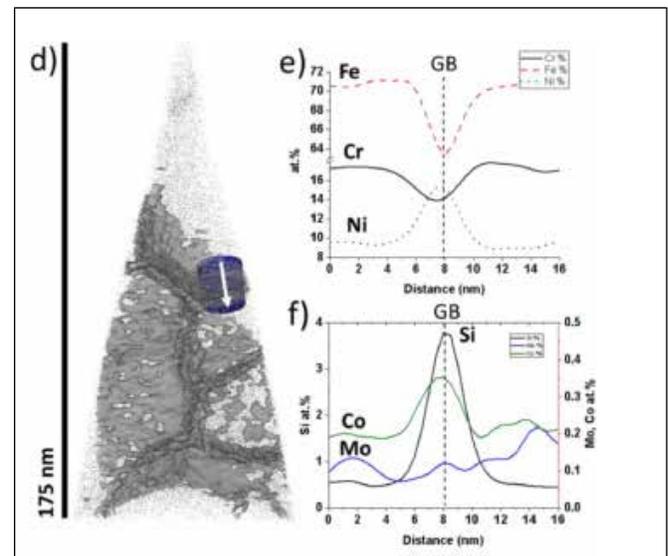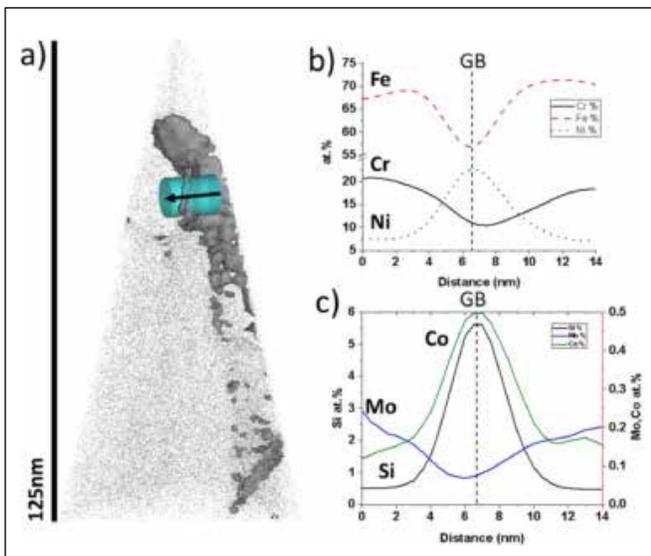
Figure 6. PED misorientation maps (left) and phase maps (right) showing γ-austenite (red) and α-ferrite (green) for (a) HPT, (b) ECAP, and (c) CG 304L ion irradiated at 500°C.

of nanostructured steels have also been completed and detailed post-irradiation microstructural characterization is being carried out. Preliminary results also indicate improved irradiation tolerance of ECAP and HPT steels as compared to their conventional CG counterparts.

Conclusions:

ECAP and HPT manufacturing produced ultrafine-grained and nanocrystalline steels (304, 316, Grade 91, and Kanthal-D), respectively. These steels have significantly higher hardness and strength compared to conventionally manufactured CG steels. Most of the UFG and NC steels are thermally stable up to 500–600°C. ECAP-manufactured steels are found to be more thermally stable than HPT manufactured ones owing to the high volume of low-angle grain boundaries stabilizing the microstructure. Ion irradiation and post-irradiation studies indicate that ECAP and HPT 304 have significantly enhanced resistance to irradiation-induced segregation and polymorphic transformation when compared to their conventionally manufactured CG counterpart. Such enhanced irradiation resistance is also anticipated for nanostructured Kanthal-D and Grade 91 steels, which will be confirmed after the current investigations are carried out. The ion irradiation studies suggest that nanostructuring using ECAP and HPT is a promising method to improve the irradiation tolerance of steels. Neutron irradiation to 2 dpa has been completed, and post-irradiation examination will be started. ECAP and HPT are promising for manufacturing alloys with improved performance for current and advanced reactors.

Si atoms (grey) and 4 at.% Si isoconcentration surface to highlight GBs, where mostly only one ultrafine grain was observed; (b) and (c) 1-D concentration profiles across the region of interest (ROI) in a) showing typical RIS behavior with enrichment in Ni, Si, Ti, and Co, and depletion in Fe, Cr, and Mo; (d) another APT reconstruction of irradiated HPT304L showing Si atoms (grey) and 2 at.% Si isoconcentration surface to highlight GBs, where only NC grains were observed; (e) and (f) 1-D concentration profiles across the ROI shown in (d), indicating that RIS was reduced in the NC grains, as compared to that in the ultrafine grains.

Irradiation Performance Testing of Specimens Produced by Commercially Available Additive Manufacturing Techniques

Jeffrey King, Ryan Collette, Mark Graham, Colorado School of Mines

Additive manufacturing (AM) technologies have the potential to significantly impact many industrial sectors, including the nuclear energy industry. These technologies manufacture parts through a variety of techniques that add material to a developing part in a controlled and reproducible fashion. Parts produced using additive techniques can be produced in nearly any shape or configuration, including many that are not possible using conventional manufacturing techniques. Thus, AM can be used to produce unique heat exchanger geometries or difficult to assemble piping unions. AM also offers the potential for quickly and affordably producing one-of-a-kind replacement parts, which can be extremely important in maintaining 40+ year-old nuclear power facilities.

Jeffrey King
Colorado School of Mines

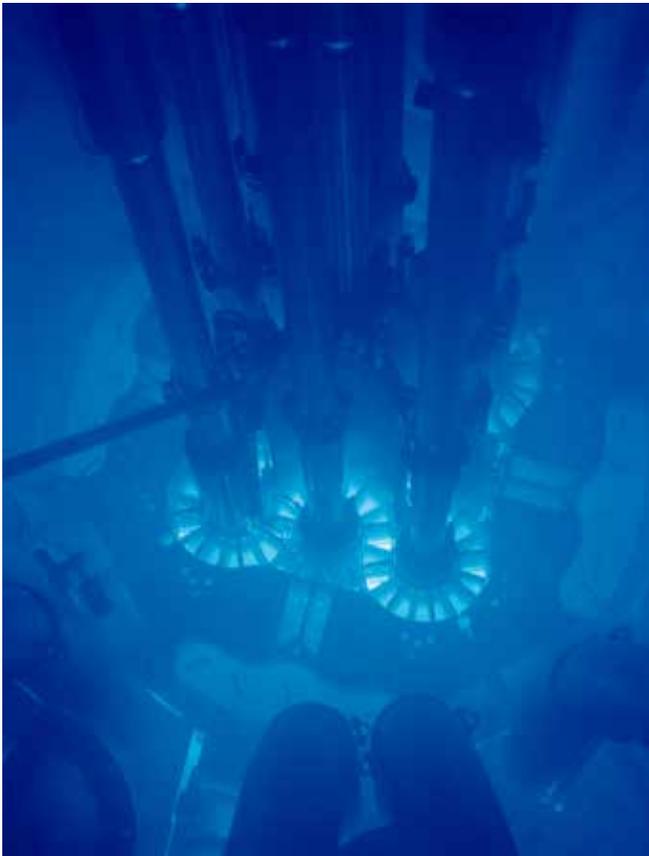Figure 2. Sub-miniature tensile test specimens.

Despite the potential benefits, the deployment of AM technologies to support the nuclear energy industry is limited by two things: (1) a lack of characterization and property data for parts produced by different AM techniques, which limit the ability of additively manufactured parts to meet nuclear quality assurance requirements; and (2) a lack of data related to the irradiation and thermal performance of AM parts, which limit confidence that these parts can survive in the challenging environments needed for nuclear energy applications.

The project will collect neutron irradiation performance data for stainless steel and Inconel specimens produced using a range of commercially available AM techniques (laser powder bed, laser free form, and electron-beam wire feed). A comparison of the physical properties and microstructure of the irradiated specimens to those of the as-fabricated specimens will provide insight into the viability of additively manufactured parts for nuclear reactor applications, identify key areas of concerns for further technology development efforts, and provide data for future computational model development.

Current Status

The Colorado School of Mines (Mines) harvested tensile bar and thermophysical property test specimens from material billets produced by a representative range of currently available AM techniques. Mines conducted pre-irradiation thermophysical and mechanical testing (tensile strength, yield strength, elastic modulus, ductility, thermal conductivity, and thermal diffusivity) and micro-structural characterization of the specimens. A subset of the specimens has been

Figure 1. Advanced Test Reactor at Idaho National Laboratory.

Continued from previous page

Figure 3. Thermal conductivity of as-manufactured and heat-treated 316L stainless steel as a function of temperature.

Figure 4. Thermal conductivity of as-manufactured and heat-treated Inconel 718 as a function of temperature.

irradiated to a range of fast neutron fluences at typical light-water reactor temperatures (~600 K) in the Advanced Test Reactor (Figure 1). The Nuclear Science Use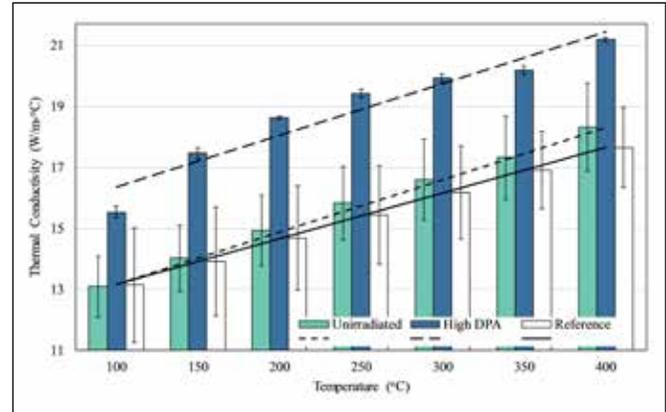r Facilities (NSUF) is preparing to ship the first round of tensile test specimens (Figure 2) to the Low Activation Materials Design and Analysis facility at Oak Ridge National Laboratory. Thermophysical property testing is underway at Idaho National Laboratory. The initial results indicate that neutron radiation results in an increase in the thermal conductivity of the additively manufactured specimens. Figures 3 and 4 show the current thermal conductivity results for laser powder bed produced 316L stainless steel and Inconel 718, respectively. The medium displacement per atom (dpa) range in Figure 3 represents specimens with doses from 0.51 to 0.67 dpa and the high dpa range in Figures 3 and 4 includes specimens with doses ranging from 1.49 to 1.63 dpa.

Recent publications on the properties of AM specimens produced by laser sintering processes indicate that these materials can exceed the strength-ductility trade-off inherent to traditionally manufactured materials. That is, AM materials can show high strength with greater ductility than conventionally produced materials as a result of the unique microstructures produced by the AM process (Figure 5). Molecular dynamics models of these structures developed at Mines indicate that these structures will also serve as effective sinks for radiation-induced defects at low doses (<2 dpa), but higher doses will tend to degrade their effectiveness. Thus, commercially available AM parts may demonstrate enhanced performance compared to conventionally manufactured parts in low-dose applications, which could likely be improved if the fabrication parameters can be tailored to promote the formation of microstructure features known to enhance radiation tolerance. Transmission electron microscopy imaging of the irradiation specimens, planned at Idaho National Laboratory, will seek to confirm or refute this hypothesis.

Conclusion

This project will provide high-value data on the performance of additively manufactured parts in a neutron radiation environment. Successful completion of the project will provide data for the qualification of additively manufactured parts for nuclear applications and may enable the development of tailored microstructures that provide enhanced resistance to radiation damage.

The NSUF continues to provide funding and facility support for this project.

Figure 5. Transmission electron microscope image of additively manufactured 316L stainless steel showing the characteristic cellular dislocation structures produced by laser sintering.

Initial Results of Irradiation Effects in PM–HIP Structural Alloys

Janelle Wharry
Purdue University,
West Lafayette, IN

Yangyang Zhao
Purdue University,
West Lafayette, IN

Caleb Clement
Purdue University,
West Lafayette, IN

Donna Guillen
Idaho National
Laboratory,
Idaho Falls, ID

David Gandy
Electric Power
Research Institute,
Charlotte, NC

Manufacturing processes have considerable influence over the safety and integrity of nuclear reactor vessels and internal components. Established processes such as casting, plate rolling and welding, forging, drawing, and extrusion have been used to fabricate structural and pressure-retaining materials used in the nuclear power industry for the past 60+ years. However, weldability and inspectability are ongoing issues in the manufacture of reactor vessels and internals. Furthermore, these components are subject to harsh service environments, which combine high-radiation fluence, high temperature, and mechanical stress. These conditions can accelerate material degradation and failure, with the most extreme degradation often occurring at weldments and in poorly manufactured or inspected components. Advanced reactor designs and lifetime extensions to the existing fleet of light water reactors (LWRs) will exacerbate materials degradation issues by increasing the duty on reactor internals. Thus, developing reliable manufacturing processes wherein high-quality weldments and inspections can be performed is of great importance to the continued safety and operation of nuclear power plants.

Recently, alloys produced by powder metallurgy with hot isostatic pressing (PM-HIP) have been developed and introduced for pressure-retaining applications in the fossil power industry [1–3]. These alloys exhibit excellent structural uniformity, no chemical segregation, superior mechanical properties, and enhanced weldability. In addition, PM-HIP components are produced in a near-net shape, which offers the distinct advantages of minimizing machining and enhancing the ease of inspectability of the component. Because of these exceptional properties,
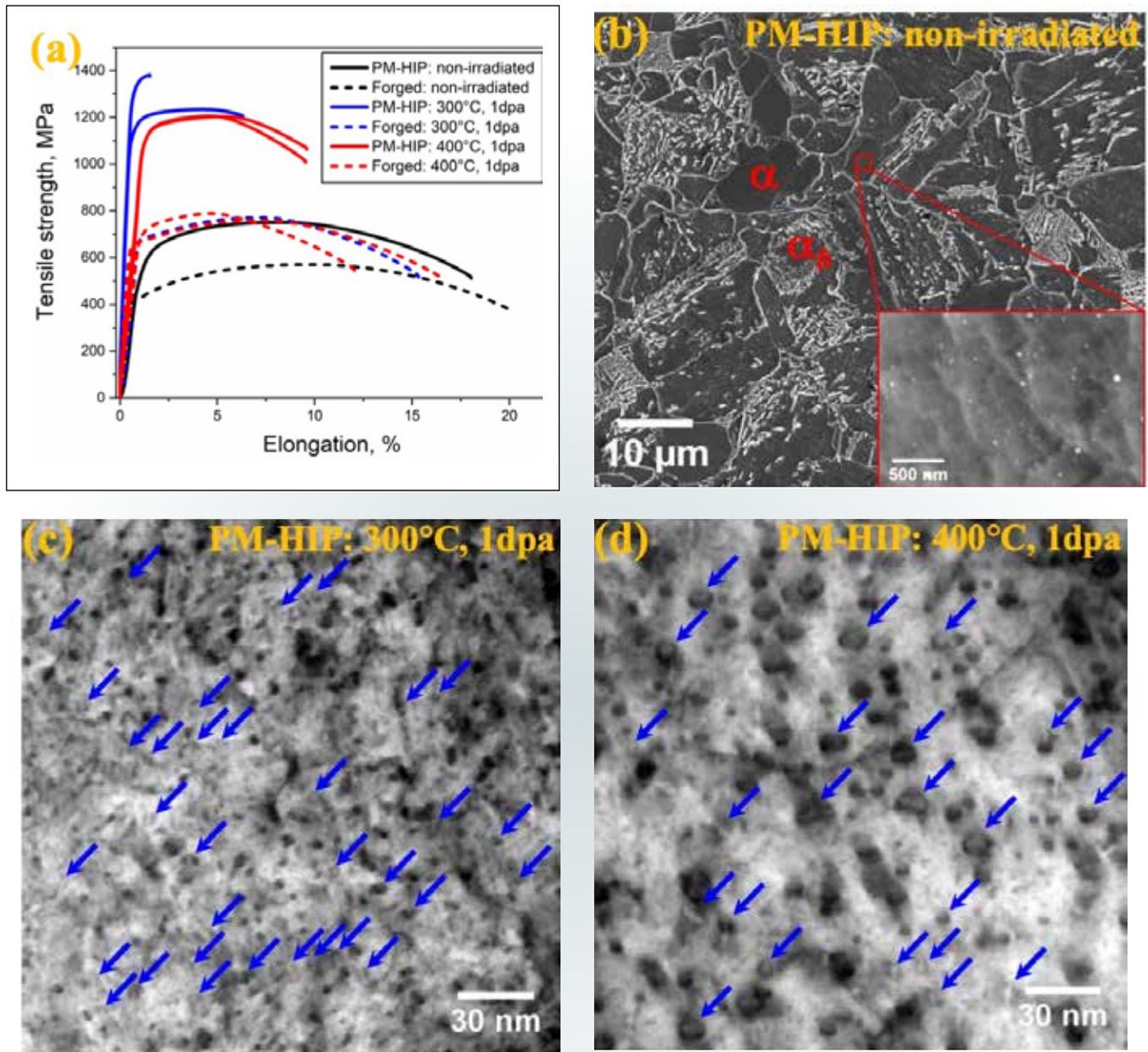
PM-HIP alloys are of interest to the nuclear power industry as potential structural materials for LWRs, advanced LWRs, small modular reactors, and advanced (e.g., Generation IV) reactors. However, little is known about the irradiation response of PM-HIP alloys, particularly in comparison to that of conventional alloys [4–8].

A Nuclear Science User Facilities project initiated in 2015 is conducting a neutron irradiation campaign to produce necessary data for qualification of various reactor structural alloys fabricated by PM-HIP. Neutron irradiations have been conducted in the Advanced Test Reactor (ATR) at Idaho National Laboratory. PM-HIP alloys were irradiated side-by-side with their conventionally fabricated counterparts to enable a direct comparison of their irradiation response. Alloys included in the study were austenitic stainless steels 304L and 316L, Ni-base alloys 625 and 690, ferritic steel Grade 91, and low-alloy steel SA508 Class 1 Grade 3. Irradiations were carried out to target temperatures of $300 \pm 50°C$ and $400 \pm 50°C$, to irradiation fluences of 1.0 and 3.0 displacements per atom (dpa), corresponding to a dose rate of $\sim0.5–1.0 \times 10\text{-}7$ dpa/sec. Specimens were inserted into the ATR in late 2017, and became available in 2019. Post-irradiation analysis commenced in late 2019. Initial results from both neutron and ion irradiations will be discussed in this article.

Amongst the ATR irradiated specimens, post-irradiation examination prioritized the SA508 pressure vessel steel. Tensile testing of neutron irradiated specimens revealed greater irradiation-induced hardening, embrittlement, and reduction in ductility in the PM-HIP SA508 than in forged
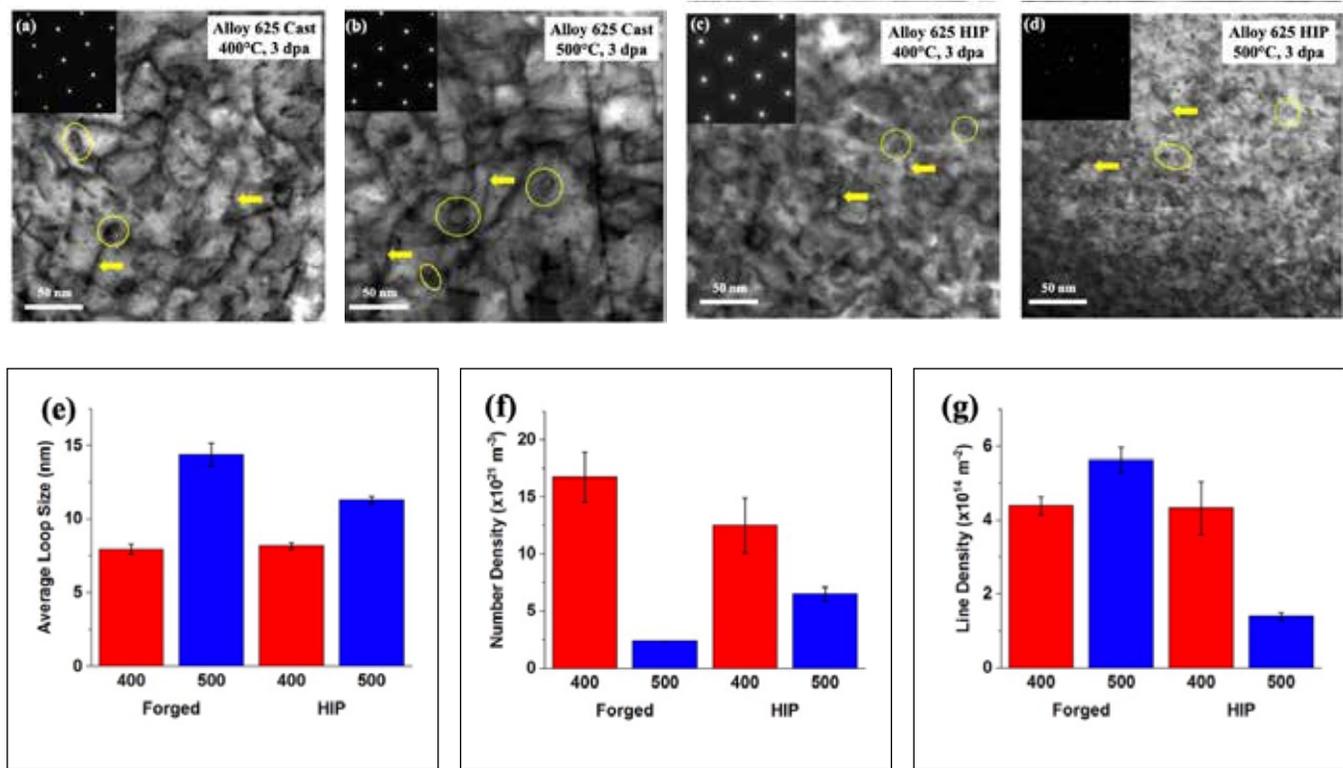
Continued from previous page

Figure 1. (a) Tensile stress-strain curves of PM-HIP and forged SA508 samples before and after neutron irradiation to 1 dpa at 300°C and 400°C; (b) SEM micrograph reveals dual-phase ferrite (α) and bainite (α_b) microstructure of the as-fabricated PM-HIP SA508, with inset spherical oxide nanoparticles uniformly distributed throughout the matrix; and [011] zone axis down-zone STEM images of irradiation-induced dislocation loops (indicated by arrows) formed in PM-HIP SA508 irradiated to 1 dpa at (c) 300°C and (d) 400°C.

SA508 (Figure 1[a]). To explain this difference in mechanical performance, the irradiated microstructures are under investigation using a combination of scanning electron microscopy (SEM), transmission electron microscopy (TEM), and atom probe tomography (APT). The as-fabricated (pre-irradiation) PM-HIP SA508 exhibits a multi-phase microstructure comprised of ferrite (denoted as α), bainite (denoted as α_b), and spherical oxide nanoparticles uniformly distributed throughout the matrix, as shown in the backscatter SEM image in (Figure 1[b]). Following irradiation, dislocation loops nucleate and are imaged using scanning TEM (STEM) down-zone axis imaging (Figure 1[c]–[d]). Typical trends are observed in which the average loop size increases with irradiation temperature, while the loop number density decreases with increasing temperature.

Figure 2. Bright field STEM imaging of dislocation loops (circled) and lines (arrows) in 100 dpa ion irradiated Alloy 625, (a) forged, 400°C, (b) forged, 500°C, (c) PM-HIP, 400°C, (d) PM-HIP, 500°C; with quantitative analysis of (e) average loop size, (f) loop number density, and (g) dislocation line density.

The dislocation loop population accounts for some of the embrittlement, but the irradiation-induced nucleation and growth of nanoprecipitates (e.g., G-phase, Cu-rich precipitates) are well known to play a key role in pressure vessel steel embrittlement. Thus, we are currently completing APT analysis of PM-HIP SA508 to investigate the evolution of irradiation-induced precipitates, as well as the pre-existing oxide nanoprecipitates. We are also in the process of completing TEM and APT analysis of irradiated forged SA508. We believe this direct comparison will help explain differences in irradiation embrittlement between the two processing methods.

In parallel to the ATR neutron irradiations, ion irradiations were also carried as a rapid and systematic scoping study. PM-HIP and wrought versions of Ni-base Alloy 625 were irradiated using 4.5 MeV Fe^{2+} ions at the Michigan Ion Beam Lab. Irradiations were conducted at 400 ± 5°C and 500 ± 5°C to a dose of 100 dpa measured at a depth of 400–700 nm from the irradiation incident surface. This corresponded to a dose rate of ~1.1–1.2 × 10^{-3} dpa/sec.

TEM lamella were fabricated from the bulk irradiated sample using focused ion beam milling. The irradiated microstructure was examined by TEM and STEM, focusing on the 400–700 nm depth below the irradiated surface. Dislocation loops and lines were imaged along the [011] zone axis using down-zone STEM imaging (see Figure 2[a]–[d]). The average loop sizes of the PM-HIP and forged Inconel 625 are statistically invariant at 400°C, but at 500°C, loops in the PM-HIP specimen are smaller than in the forged specimen (see Figure 2[e]). The loop number density is higher in the forged material than in the PM-HIP at 400°C, although this trend reverses at 500°C (see Figure 2[f]). Dislocation line density remains relatively unchanged with irradiation (see Figure 2[g]), although some lines are annealed from the PM-HIP specimen after 500°C irradiation. No voids were observed under any of the irradiation conditions.

These results from ion irradiation of Alloy 625 suggest that irradiated microstructure development in the PM-HIP alloy may be less sensitive to temperature than is the forged material. This could make PM-HIP components particularly well-suited for nuclear reactors that undergo thermal cycling and transients (e.g., Transient Reactor Test [TREAT] Facility), and for components susceptible to thermal excursions during off-normal operations.

AMM-SBIR Projects

Real Time Non–Destructive Evaluation during 3D Manufacturing of Metal Parts

Araz Yacoubian
Ler Technologies, Inc.

Gary Winter
Ler Technologies, Inc.

Paul LoVecchio
Ler Technologies, Inc.

Additive manufacturing, such as laser sintering or melting of additive layers, can produce parts rapidly at small volume and in a factory setting. To make the parts nuclear quality, a real-time non-destructive evaluation (NDE) technique is required to detect defects while they are being manufactured. The NDE technique is a sensor unit that is incorporated in a direct metal laser sintering machine to capture defects in real time. The sensor data can be used to identify defects as they occur so that immediate corrective action can be taken. It also provides parameters that enable the prediction if the part is of nuclear quality. The final outputs of the sensor unit produce a defect map in real time as the part is being printed. Defects are revealed, such as voids improper melting, bulging of the metal, and out-of-spec prints.
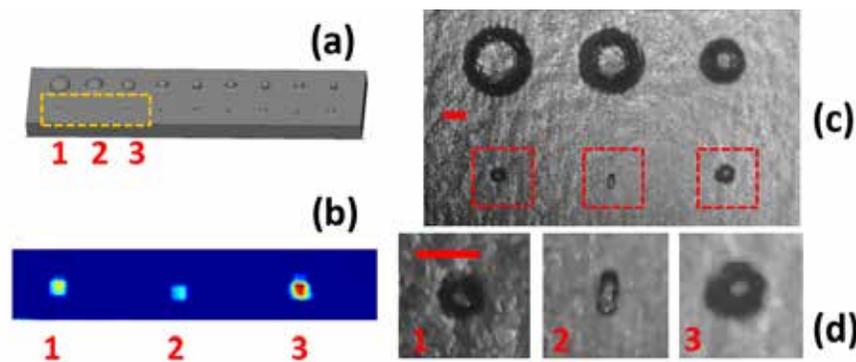
Results and Current Status

Samples with representative defects that occur during additive manufacturing, such as direct metal laser sintering (DMLS), have been designed and fabricated. Materials include stainless steel 316 samples and Inconel-718.
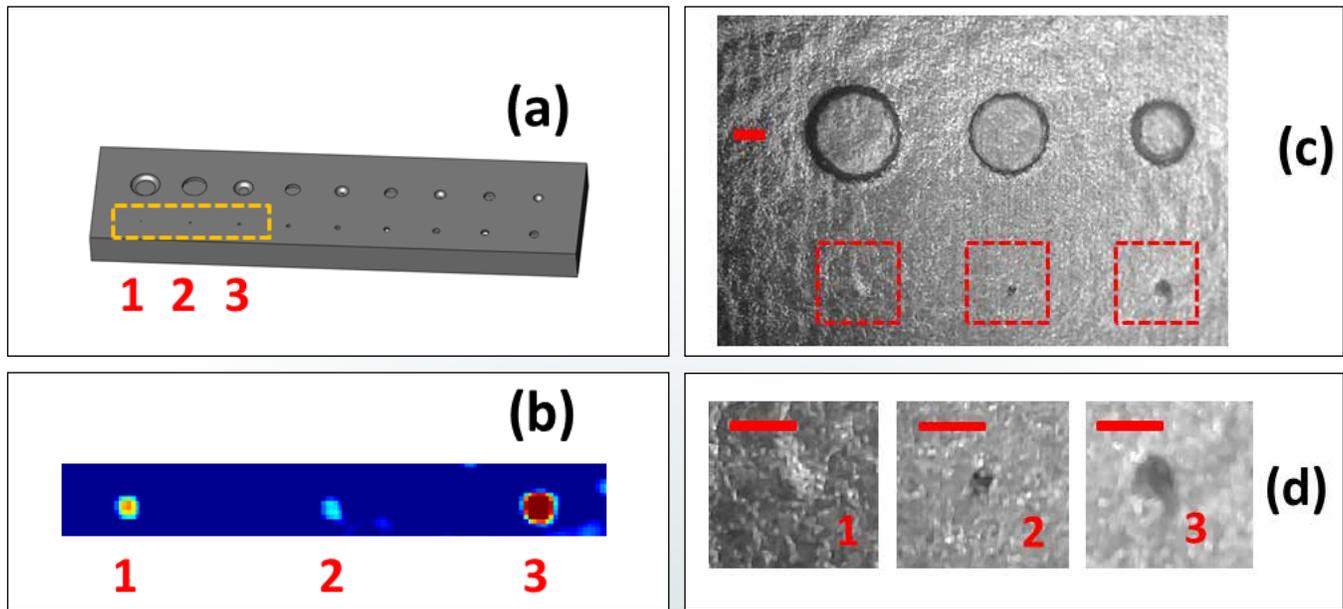
The samples were tested using the NDE approach. The data obtained from the tests revealed the defects that matched on the samples and demonstrated the robustness of using multiparameter NDE approach. A defect detection example is shown in Figure 1 for material bulging detection on a DMLS-printed stainless steel 316 sample. The sample included an array of defects of various sizes and shapes. The sample was designed and a 3D CAD layout was generated, as shown in Figure 1a. The samples were tested and the sensor output is shown in Figure 1b, detecting the smallest defects marked 1, 2, and 3 in the sample. As a comparison, Figures 1c and 1d show a microscope image of the sample, with the smallest defects marked 1 to 3, corresponding to the defects detected by the sensor as shown in Figure 1b.

Figure 1. (a) CAD layout of a sample with bulging defects; (b) sensor output showing defects 1, 2, and 3; (c) microscope image of direct metal laser sintering (DMLS) fabricated sample containing three defects of different sizes; (d) details of the defects. Red scale bars in (c) and (d) are 1 mm.

Figure 2. (a) CAD layout of a void sample; (b)sSensor output showing defects 1, 2, and 3; (c) microscope image of direct metal laser sintering (DMLS) fabricated sample containing three defects of different sizes; (d) details of the defects. Defects that are difficult to see even with a microscope are revealed with the sensor. Red scale bars in (c) and (d) are 1 mm.

Another example of void detection on a DMLS printed stainless steel 316 sample is shown in Figure 2. The sample included an array of defects of various sizes and shapes. A 3D CAD layout of the sample is shown in Figure 2a. Sensor output illustrating detection of the smallest defects on the sample defects marked 1, 2 and 3 is shown in Figure 2b. Figures 2c and 2d show a microscope image of the sample, with the smallest defects marked 1 to 3, corresponding to the defects detected by the sensor shown in Figure 2b. The smallest defects are difficult to see even with a microscope and are successfully detected by this NDE approach.

One of the challenges of real-time defect detection in metal printing environment is the presence of various types of noise. To ensure that the proposed approach is suitable for this environment, work was performed and noise reduction was successfully demonstrated via set of simulations and experiments.

Currently, a table-top prototype is being tested utilizing samples of various representative defects. Output generated from the sensor will be utilized to generate a defect map in real time.

Impact and Value

When this NDE technology is commercialized, the sensor unit will be incorporated in the 3D printing machines without requiring hardware design changes to the machine. The sensor data will be utilized to pre-qualify parts for nuclear quality; therefore, the data will minimize or eliminate the need for post-fabrication testing. The economic benefits include reduction of cost of post-process testing, and significant reduction of loss of labor and material due to faulty parts. DOE and other branches of the government will benefit by streamlining the nuclear parts manufacturing. The reduced cost of manufacturing will help transition to modern nuclear energy, which will benefit the public by providing safe and cost-effective energy solution. Additionally, utilizing this technology potentially results in higher quality 3D parts due to advanced inspection.

Additive Manufacturing of Nuclear Fuel Assembly End Fittings and Associated Components

George Pabis
Innovative
Technologies
International, Inc.

Lauren Gramlich
Innovative
Technologies
International, Inc.

Manufacturing technologies are ever-evolving, but the nuclear industry has not taken full advantage of these new technologies. One such technology that has lagged behind is additive manufacturing (AM). AM offers many advantages, including decreased part count, intricate geometries that are not manufacturable by other methods, improved performance, and cost savings. With the high cost of building new nuclear reactors, exploring AM for nuclear reactor components is of great importance.

Background

NovaTech has been awarded three United States Department of Energy (U.S. DOE) Small Business Innovative Research Phase II grants over the past several years. These projects have focused on AM top- and bottom-end fittings for both pressurized water reactors (PWRs) and boiling water reactors (BWRs), and hold-down springs for small modular reactors (SMRs). NovaTech has successfully additively manufactured bottom nozzles and lower tie plates while combining multiple parts and improving performance. Additionally, an improved hold-down spring had been designed and is currently being integrated in the top nozzle design.

PWR Bottom Nozzles

The AM bottom nozzle project successfully produced a full-scale, functioning bottom nozzle. This bottom nozzle is shown in Figure 1 and features a design that does not require a bottom-end grid or P Grid. The AM nozzle is fabricated with features that position and lock the fuel rods in the bottom nozzle while still allowing fuel rod reconstitution. A torturous path debris filter is also built into the bottom nozzle and includes a lower skirt and smaller LOCA communication holes to prevent debris from migrating to the gap between fuel assemblies. Rounded and blended corners are also included
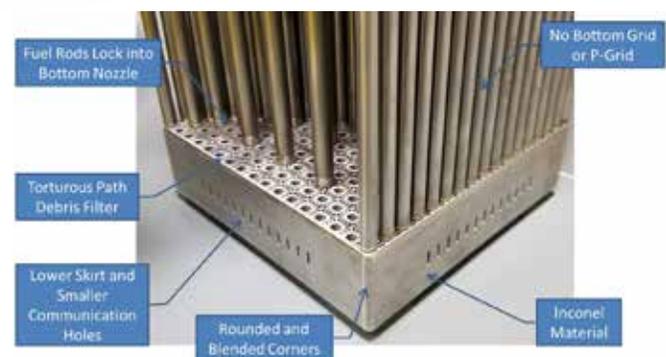
in the design to improve handling interfaces and reduce the possibility of damage during fuel handling. All of this was accomplished while keeping the overall cost comparable to the existing combined cost of the parts that the design replaces. This project concluded in March 2020.

SMR Hold-down Springs

The SMR hold-down spring project is ongoing and is scheduled to be completed by the end of the year. Existing hold-down springs are usually coil springs or leaf springs, depending on the fuel assembly design. The AM hold-down spring that NovaTech is designing is intended to be a single-piece replacement for the 3-leaf Westinghouse-style spring.

Efforts are currently focused on optimizing the load-deflection curve to match the curve produced by the existing 3-leaf design while minimizing material strain. Surface finish optimization is also a focus of this project as the springs undergo high strains, which can make them

Figure 1. Additive manufactured PWR bottom nozzle.
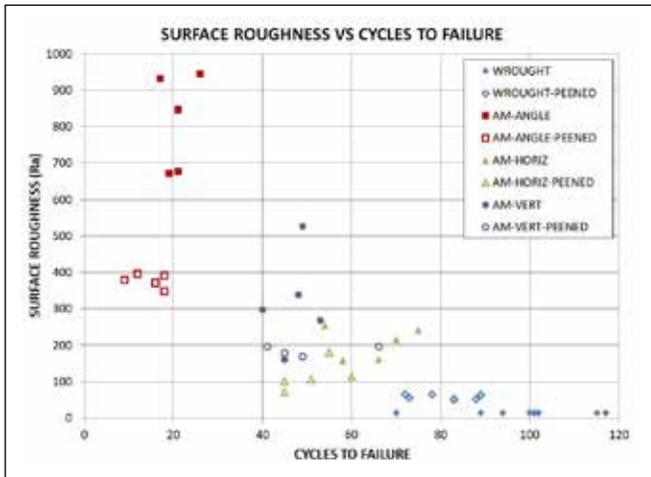
Continued from previous page

Figure 2. Prototype additive manufactured SMR hold-down spring load-deflection curves.
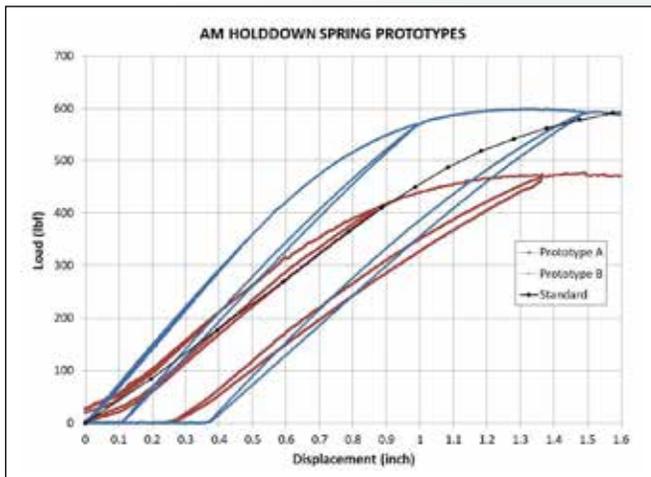

Figure 3. AM low-cycle fatigue data.

susceptible to stress corrosion cracking (SCC). To date, both laser and EB powder bed AM processes have been evaluated as well as shot peening and grinding post processes. Additional post processing methods are being evaluated.

Multiple AM hold-down spring prototypes have been fabricated to determine the best AM process and the best part orientation in an AM machine. These spring prototypes have been load tested (see Figure 2) and the data from these tests has been used to optimize the ANSYS and LS-Dyna spring models and their associated material stress-strain curves.

Low-cycle fatigue (LCF) tests are also being performed to evaluate the effects of surface finish, heat treatment, and post processing techniques (see Figure 3). SCC specimens are currently being prepared that will be placed in an autoclave to compare the performance of wrought specimens to AM specimens. The results from these efforts will be a single-piece AM hold-down spring that has been optimized for the 3-leaf Westinghouse-style fuel assembly.

Figure 4. Monolithic additive manufactured BWR lower tie plate.

BWR Lower Tie Plate

Current BWR lower tie plate designs are welded from several parts and machined: a cast nose piece, a machined tie plate, formed channel seal springs, and in some designs a machined filter plate. This lengthy process is expensive, and costs can be reduced by combining all of these components into one piece and manufacturing with AM. An AM monolithic 10×10 lower tie plate is shown in Figure 3.

In addition to reducing part count, another goal for the BWR lower tie plate project is to improve debris filtering capabilities. Fuel rod failures can occur if debris (usually in the form of small wires and metal shavings), get caught in the spacer grids and wear a hole in the fuel rod, so minimizing debris that flows through the lower tie plate is vital. However, it is also critical that the pressure drop across the lower tie plate is maintained, as this can vary between reactor designs. Using a similar torturous path design to that of the PWR bottom nozzle design, the pressure drop can be fine-tuned, while also reducing the likelihood of debris passing through the filter plate.

Conclusions

NovaTech is excited about the potential that AM can bring to the nuclear industry to increase performance and reduce cost. As the AM designs are completed, NovaTech looks forward to sharing the results with the AM and nuclear communities.

Acknowledgments

PROGRAM AWARDS
AMM Publications and Presentations

Journal Publications:

1. Duan, J. Q., Wen, H. M.*, Zhou, C. Z., He, X. Q., Islamgaliev, R. K., Valiev, R. Z., "Discontinuous grain growth in an equal-channel angular pressing processed Fe-9Cr steel with a heterogeneous microstructure," *Materials Characterization*, Vol. 159, 2020, p. 110004 (*Corresponding author).

2. Duan, J. Q., H. M.Wen*, C. Z. Zhou, X. Q. He, R. K. Islamgaliev, R. Z. Valiev, "Annealing behavior in a high-pressure torsion-processed Fe–9Cr steel," *Journal of Materials Science*, Vol. 55, 2020, pp. 7958–7968 (*Corresponding author).

3. Hoffman, A. K., M. Arivu, H. M.Wen*, L. He, K. Sridharan, X. Wang, W. Xiong, X. Liu, L. F. He, Y. Q. Wu, "Enhanced Resistance to Irradiation Induced Ferritic Transformation in Nanostructured Austenitic Steels," *Materialia*, Vol. 13, 2020, p. 100806.

4. Yeom, H., and K. Sridharan "Recent advances of cold spray technology in nuclear energy applications," *Advanced Materials and Processes*, (invited), July 2020.

5. H. Yeom and K. Sridharan, "Cold Spray Technology in Nuclear Energy Applications: A Review of Recent Advances," *Annals of Nuclear Energy* (accepted in press 2020), January 2021, Vol. 150, p. 107835, DOI: 10.1016/j.anucene.2020.107835

6. Wang, X., Y. Gao, M. McDonnell, Z. J. Feng, "On the solid-state-bonding mechanism in friction stir welding," *Extreme Materials Letters*, 2020, Vol. 37, p. 100727.

Conferences and Proceedings:

1. Collette, R., J. King, B. Amin-Ahmadi, "TEM Analysis of Additively Manufactured Stainless Steels Prior to Neutron Irradiation," *Transactions of the American Nuclear Society*, 2019, Vol. 121, pp. 592–595, doi: 10.13182/T30913.

2. Graham, M., and J. King, "Neutron Irradiation Effects on Additively Manufactured Stainless Steels and Inconels - Pre-Irradiation Thermophysical Property Testing," *Transactions of the American Nuclear Society*, 2019, Vol. 121, pp. 599–602, doi: 10.13182/T31172.

3. Graham, M., Becquet, C., and King, J., "Neutron Irradiation Effects on Additively Manufactured Stainless Steels and Inconels - Pre-Irradiation Mechanical Testing," *Transactions of the American Nuclear Society*, 2019, Vol. 121, pp. 596–598, doi: 10.13182/T31169.

4. Caleb D. Clement, Xiang Liu, David W. Gandy, and Janelle P. Wharry, "Ion irradiation effects on the microstructure of PM-HIP Inconel 625," *2020 TMS Annual Meeting*, San Diego California, February 2020.

5. Wen, H. M., A. K. Hoffman, J. Q. Duan, M. Arivu, "Ultrafine-grained and nanocrystalline steels for enhanced mechanical properties and irradiation resistance," presentation, *2020 TMS Annual Meeting*, San Diego, California, February 23–27, 2020.

6. Hoffman A. K., M. Arivu, H. M. Wen, "Severe Plastic Deformation Enhanced Segregation and Precipitation in Nanostructured Steels," presentation, *2020 TMS Annual Meeting*, San Diego, California, February 23–27, 2020.

7. Hoffman A. K., M. Arivu, H. M. Wen, "Enhanced Austenite Stability in Nanostructured Steels During Ion Irradiation," *2020 TMS Annual Meeting*, San Diego, California, February 23–27, 2020.

8. Arivu M, A. K. Hoffman, J. Q. Duan, H. M. Wen, "Thermal stability of nanostructured ferritic and austenitic stainless steels," presentation, *2020 TMS Annual Meeting*, San Diego, California, February 23–27, 2020.

9. Wen H. M., "Development, manufacturing and characterization of nanostructured materials for structural applications in extreme environments," invited talk, Department of Materials Science and Engineering, University of California, Los Angeles, January 24, 2020.

10. X. Zhang, J. Saniie, A. Heifetz, "Neural learning based blind source separation for detection of material defects in pulsed thermography images," accepted at *IEEE Conference on Electro-Information Technology* (EIT 2020).

11. A. Heifetz, D. Shribak, T. Liu, T. Elmer, P. Kozak, S. Bakhtiari, B. Khaykovich, W. Cleary, "Pulsed thermal tomography nondestructive evaluation of additively manufactured reactor structural materials," *Transactions of the American Nuclear Society*, Vol. 121, No. 1, 2019, pp. 589–591.

12. Graham, J., M. Lenling, H. Yeom, P. Hosemann, and K. Sridharan, "Evaluation of Cold-Sprayed 14YWT," *The Metallurgical Society (TMS) Annual Conf., Symposium on Additive Manufacturing for Energy Applications II, San Diego, California*, February 2020.

13. Yeom, H., M. Lenling, T. Dabney, J. Graham, P. Hosemann, D. Hoelzer, S. Maloy, and K. Sridharan, "Manufacturing Oxide Dispersion Strengthened (ODS) Steel Fuel Cladding Tubes by Cold Spray Technology," *The Metallurgical Society (TMS) Annual Conf., Symposium on Additive Manufacturing for Energy Applications II, San Diego, California*, February 2020.

14. W. Xiong, "CALPHAD-based ICME Design for Additive Manufacturing: Successes and Challenges," *Symposium on Additive Manufacturing for Energy Applications II, San Diego, California*, February 23–27, 2020.

Continued from previous page

Workshops and Technical Meetings

1. Gandy, D., "Presentation on Factory Fabrication of SMR and AR Vessel Assemblies," *GIF AMME Workshop on Advanced Manufacturing, Paris France*, February 18–19, 2020.

2. Van Rooyen I. J., and M Messner, "Presentation an Overview: Advanced Manufacturing Collaboration in the USA," *GIF AMME Workshop on Advanced Manufacturing, Paris France*, February 18–19, 2020.

3. Gandy, D., "Presentation on Advanced Manufacturing Methods (AMM) for SMRs/ARs," *NRC-EPRI Quarterly Update on SMR Manufacturing and Fabrication*, July 16, 2020.

4. Gandy, D., Presentation on Powder Metallurgy-HIP for SMRs and Advanced Reactors, ASME Boiler Pressure Vessel Code Meetings—Task Group Div. 5, May 11, 2020.

5. Gandy, D., "Presentation on Factory Fabrication of Small Modular Reactor Vessel Assemblies," *EPRI Nuclear Power Council Meetings,* February 2020.

6. Gandy, D., S. Tate, M. Albert, C. Armstrong, W. Cleary, "Presentation on 316L Stainless Steel Manufactured via Laser Powder Bed Fusion—Additive Manufacturing," *ASME Boiler Pressure Vessel Code Meetings*—Section III MF&E, August 19, 2020.

7. Gandy, D., S. Tate, M. Albert, C. Armstrong, W. Cleary, "Data Package for 316L Stainless Steel Manufactured via Laser Powder Bed Fusion Additive Manufacturing," Submitted to *ASME Boiler Pressure Vessel Code—Section III MF&E*, August 19, 2020.

8. Gramlich, *2020 Fall TechConnect Innovation Summit & Showcase, National Harbor, Maryland*, November 17–19, 2020

9. Gandy, D., S. Tate, M. Albert, C. Armstrong, W. Cleary, "DRAFT Code Case for 316L Stainless Steel Manufactured via Laser Powder Bed Fusion Additive Manufacturing," Submitted to *ASME Boiler Pressure Vessel Code—Section III MF&E*, August 19, 2020.

Future Publications and Presentations to look out for!

1. X. Zhang, J. Saniie, W. Cleary, A. Heifetz, "Detection of defects in additively manufactured stainless steel 316L with compact infrared camera and machine learning algorithms," submitted to JOM special issue on Additive Manufacturing for Energy Applications (2020).

2. A. Heifetz, D. Shribak, X. Zhang, J. Saniie, T. Liu, J.G. Sun, T. Elmer, S. Bakhtiari, W. Cleary, "Thermal tomography 3D imaging of additively manufactured metallic structures," submitted to AIP Advances (2020).

3. X. Zhang, J. Saniie, W. Cleary, A. Heifetz, "Quality control of additively manufactured metallic structures with machine learning of thermography images," submitted to JOM special issue on Machine Learning Applications in Advanced Manufacturing Processes (2020).

4. Janelle P. Wharry, Caleb D. Clement, Donna P. Guillen, Yaqiao Wu, and David W. Gandy. "Role of processing method on irradiation response of nuclear structural alloys," *International Conference on Processing & Manufacturing of Advanced Materials (THERMEC) 2020*, Vienna, Austria, rescheduled to June 2021 (abstract accepted).

5. Yangyang Zhao, Caleb D. Clement, Shujuan Wang, Yaqiao Wu, Katelyn Wheeler, Donna P. Guillen, David W. Gandy, and Janelle P. Wharry. "Neutron irradiation response of SA 508 pressure vessel steel prepared by powder metallurgy and hot isostatic pressing," *TMS Annual Meeting, Orlando Florida*, scheduled March 2021 (abstract accepted).

6. Caleb D. Clement, Yangyang Zhao, Shujuan Wang, Yaqiao Wu, David W. Gandy, and Janelle P. Wharry, "Dose and temperature dependence of microstructure and mechanical properties in ion-irradiated PM-HIP Inconel 625," *TMS Annual Meeting, Orlando Florida*, scheduled March 2021 (abstract accepted).

7. S Maloy, "Laser Additive Manufacturing of Grade 91 Steel for Affordable Nuclear Reactor Components with Improved Radiation Tolerance," Presentation abstract accepted for *TMS 2021 Annual Meeting*.

8. A. Heifetz, Z. Fisher, D. Shribak, "Detection of defects in additively manufactured metals using thermal tomography," submitted to *TMS 2021 Annual Meeting*, 2020, Additive Manufacturing for Energy Applications III.

9. Yacoubian, Submitted abstract to 2021 *TMS Annual Meeting & Exhibition, Symposium, Additive Manufacturing for Energy Applications III.*